Bachelor Project

Czech Technical University in Prague

F3

Faculty of Electrical Engineering
Department of Circuit Theory

Measurement and modelling of fundamental characteristics of the human visual system under non-standard conditions

Měření a modelování charakteristik lidského zrakového systému za nestandardních podmínek

Stepan Gorichev

Supervisor: Ing. Karel Fliegel, Ph.D.
Field of study: Medical Electronics and Bioinformatics
May 2024

ZADÁNÍ BAKALÁŘSKÉ PRÁCE

I. OSOBNÍ A STUDIJNÍ ÚDAJE

Příjmení: **Gorichev** Jméno: **Stepan** Osobní číslo: **507794**

Fakulta/ústav: **Fakulta elektrotechnická**

Zadávající katedra/ústav: **Katedra teorie obvodů**

Studijní program: **Lékařská elektronika a bioinformatika**

II. ÚDAJE K BAKALÁŘSKÉ PRÁCI

Název bakalářské práce:

Měření a modelování charakteristik lidského zrakového systému za nestandardních podmínek

Název bakalářské práce anglicky:

Measurement and modelling of fundamental characteristics of the human visual system under non-standard conditions

Pokyny pro vypracování:

Podejte přehled současného stavu v oblasti psychovizuálních experimentů vedoucích k získání základních charakteristik lidského vizuálního systému HVS (Human Visual System) a souvisejících modelů. Zaměřte se zejména na problematiku kolorimetrie a vnímání barevných rozdílů za nestandardních světelných podmínek. S využitím vhodného programového prostředí a technického vybavení navrhněte nástroje pro realizaci vybraných psychovizuálních experimentů. Ověřte funkčnost systému na základě experimentu se skupinou pozorovatelů a porovnejte výsledky pomocí dostupných modelů.

Seznam doporučené literatury:

[1] Nagai T., Kakuta K., Yamauchi Y., Luminance dependency of perceived color shift after color contrast adaptation caused by higher-order color channels, Journal of Vision, 2022.
[2] Luo M.R., Xu Q., Pointer M., Melgosa M., Cui G., Li C., Xiao K., Huang M., A comprehensive test of colour-difference formulae and uniform colour spaces using available visual datasets, Color Research and Application, 2023.
[3] De Fez M. D., Luque M. J., Viqueira V., Enhancement of contrast sensitivity and losses of chromatic discrimination with tinted lenses, Optometry and Vision Science, 2002.

Jméno a pracoviště vedoucí(ho) bakalářské práce:

Ing. Karel Fliegel, Ph.D. katedra radioelektroniky FEL

Jméno a pracoviště druhé(ho) vedoucí(ho) nebo konzultanta(ky) bakalářské práce:

Datum zadání bakalářské práce: **06.02.2024** Termín odevzdání bakalářské práce: **24.05.2024**

Platnost zadání bakalářské práce: **21.09.2025**

Ing. Karel Fliegel, Ph.D.	doc. Ing. Radoslav Bortel, Ph.D.	prof. Mgr. Petr Páta, Ph.D.
podpis vedoucí(ho) práce	podpis vedoucí(ho) ústavu/katedry	podpis děkana(ky)

III. PŘEVZETÍ ZADÁNÍ

Student bere na vědomí, že je povinen vypracovat bakalářskou práci samostatně, bez cizí pomoci, s výjimkou poskytnutých konzultací. Seznam použité literatury, jiných pramenů a jmen konzultantů je třeba uvést v bakalářské práci.

. Datum převzetí zadání

Podpis studenta

Acknowledgements

Here I would like to express my deepest obligation to my supervisor, Ing. Karel Fliegel, Ph.D., for his continuous support and guidance which helped me to finish this work.

I would also like to thank the CTU, particularly the Department of Radioelectronics for providing all the necessary technical equipment used in the practical part of this work.

Likewise I would like to thank my family for their help and belief.

Declaration

I hereby declare that the following work is the product of my own labour and I have cited all the sources I had used in the bibliography.

In Prague, 23 May 2024

Abstract

The human visual system (HVS) makes it possible to receive and process information under a wide range of colour, brightness, and spatio-temporal frequency conditions. We conducted an analysis of the theory explaining the mechanisms that allow the HVS to adapt to changes in the presented stimulus. The primary aim of this thesis is to analyze the colourimetric characteristics of the HVS under different conditions and to describe the possibilities of measuring them through psychovisual experiments. In the empirical part of the thesis, a tool was developed to conduct such experiments with a group of observers. A pilot experiment was organized to assess the performance of the program and to compare its results with the models described in the theoretical part.

Keywords: Human visual system, Colour difference, Colour space, Uniform Colour Space, Psychovisual experiment, Colourimetry

Supervisor: Ing. Karel Fliegel, Ph.D. Prague, Technická 1902/2, 166 27

Abstrakt

Lidský zrakový systém (HVS) umožňuje přijímat a zpracovávat informace v širokém spektru barevných, jasových a frekvenčních podmínek. Provedli jsme analýzu teorie vysvětlující mechanismy, které umožňují HVS přizpůsobit se změnám v prezentovaném podnětu. Primárním cílem této práce je analýza kolorimetrických vlastností HVS a popis možností jejich měření pomocí psychovizuálních experimentů za různých podmínek. V empirické části práce byl vyvinut nástroj umožňující provádět takové experimenty se skupinou pozorovatelů. Byl uspořádán pilotní experiment k posouzení výkonu programu a ke srovnání jeho výsledků s modely popsanými v teoretické části.

Klíčová slova: Lidský zrakový systém, Barevný rozdíl, Barevný prostor, Uniformní barevný prostor, Psychovizuální experiment, Kolorimetrie

Překlad názvu: Měření a modelování charakteristik lidského zrakového systému za nestandardních podmínek

Contents

Figures

Tables

Chapter 1

Introduction

The human visual system exhibits remarkable adaptability across a wide range of luminance levels, from the bright conditions of photopic vision to the dim settings of scotopic vision, with mesopic vision occupying the intermediate range. While for undertaking most of everyday tasks the HVS only engages photopic vision mechanisms, domains appear in the modern world where some special applications require mesopic vision to be involved, which is why it becomes interesting and important to examine the relations between the former and the latter. An example of such a special application could be digital cinema, where the values of intensity sometimes reach the mesopic range [12].

The following thesis aims to examine the human visual system's fundamental characteristics and options for their measurement under both standard and non-standard conditions by combining theoretical research with empirical measurements. The presented thesis mainly focuses on the colourimetry trying to comprehensively analyze what is colour and how is it perceived along various luminance levels.

The main sections of the following thesis are:

- HVS section: discusses the basics of human vision and the cells engaged in its activity. Section 2.1
- Section devoted to the colour as a concept: its perception by the HVS, colour representation methods regarding modern technology and colour assessment metrics. Section 2.2
- Section devoted to the psychovisual experiments established to measure HVS characteristics, considering colourimetry mostly. Section 2.3
- Section devoted to the tool designed and proposed for conducting psychovisual experiments with multiple observers and assessing the HVS's response to colourimetric change of the presented stimuli under various luminance conditions. Section 3.1
- Section devoted to the conducting of the pilot experiment to demonstrate the functionality and stable performance of the proposed tool. Section 4
- Conclusion of the thesis with the evaluation of the work done. Section 5

Chapter 2

Conceptual basis

This chapter lays out the theoretical framework and essential conclusions derived from recent studies, which are instrumental in establishing an understanding of how human visual system is designed regarding its ability to perceive colour, lightness and spatio-temporal frequency changes in the presented stimuli under various luminance conditions. The main point of this chapter is to asses different techniques and underline previous work in the field to provide a state-of-art review for further experiment.

2.1 Human visual system

Human visual system (HVS further) is a complicated mechanism that allows people to perceive, convey and interpret visual information. HVS is able to assess multiple complex parameters of presented stimuli such as colour, contrast, movement speed etc. Its individual functions may be abstracted as characteristics to measure which psychovisual experiments are conducted.

2.1.1 HVS regarding different types of vision

The HVS operates optimally across a spectrum of illumination, facilitated by rods and cones (see Fig. 2.1). Cones are differentiated into S, M, and L types, each sensitive to specific wavelengths, thus underpinning the colour discrimination capability of the HVS [36, 37].

Photopic vision, prevalent in high illumination, engages cone receptors, enabling colour vision and high spatial resolution.

Scotopic vision occurs under low illumination, where rod receptors, predominant in number, facilitate light sensitivity at the expense of colour vision and spatial resolution. Rods, singular in type, do not contribute to colour vision but enhance sensitivity to low-light conditions [2].

Mesopic vision encompasses the transition between photopic and scotopic vision, involving both rods and cones. This intermediary state challenges visual processing due to the dual input, affecting sensitivity, acuity, and colour discrimination [36, 2].

The luminance ratios for all the mentioned vision modes are defined by the CIE 191:2010 report [15] as follows:

- Scotopic: $L < 0.005$ cd/m^2;
- Mesopic: $L \in [0.005; 5]$ cd/m^2;
- Photopic: $L > 5$ cd/m^2.

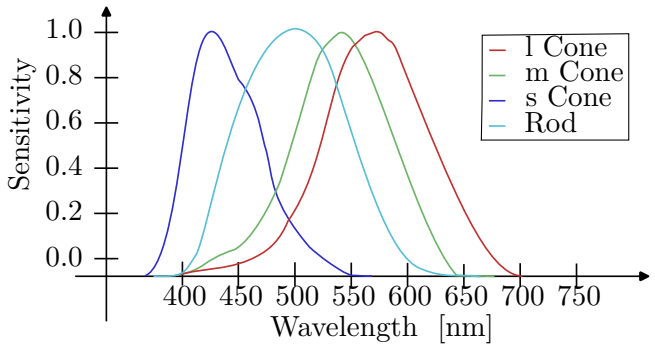

Figure 2.1: Individual photoreceptor cells' responses in relation to the wavelength of the stimuli (As per [37]).

2.2 Colour representation, recognition and distinguishing

This section deals with how colour is being encoded and displayed in modern systems and how it correlates with it's perception by the HVS.

2.2.1 Colour representation

Colour, as it was mentioned above, is an extremely important concept as well as ability to perceive or distinguish between multiple colours is very important in the human visual system. However, since the concept of colour is subjective, it requires introduction of a unified colour system, also known as colour space, for colourimetric evaluation and further possible psychovisual experiments. There are several such systems, which we will explore in the following sections.

CIE colour spaces

The Commission Internationale de l'Eclairage (CIE) colour spaces represent a comprehensive system for quantifying human colour perception, offering a mathematical model for colour representation that covers the entire visible spectrum. Since human eye has three types of colour sensors (LMS), each representative for certain wavelengths, it seems to be logical that colour should be defined by three parameters and therefore colour space must be three-dimensional. One of the colour spaces the depicts this idea is the CIE XYZ colour space. XYZ are tristimulus values, parameters that quantify the perceived colour in terms of three primary colours and luminance (Y).

The relation between LMS cones responses and XYZ values is given by the Hunt-Pointer-Estevez matrix [22]:

$$\begin{bmatrix} X \\ Y \\ Z \end{bmatrix} = \begin{bmatrix} 1.91020 & -1.11212 & 0.20191 \\ 0.37095 & 0.62905 & 0 \\ 0 & 0 & 1.000 \end{bmatrix} \begin{bmatrix} L \\ M \\ S \end{bmatrix}_{HPE} . \tag{2.1}$$

The derivatives of this colour space are CIE 1931 colour space chromaticity diagram and CIE 1976 UCS diagram (see Fig. 2.2), both of which aimed to divide colour representation task into two parts: brightness and chromaticity, and then represent colour by its chromaticity for given luminance levels.

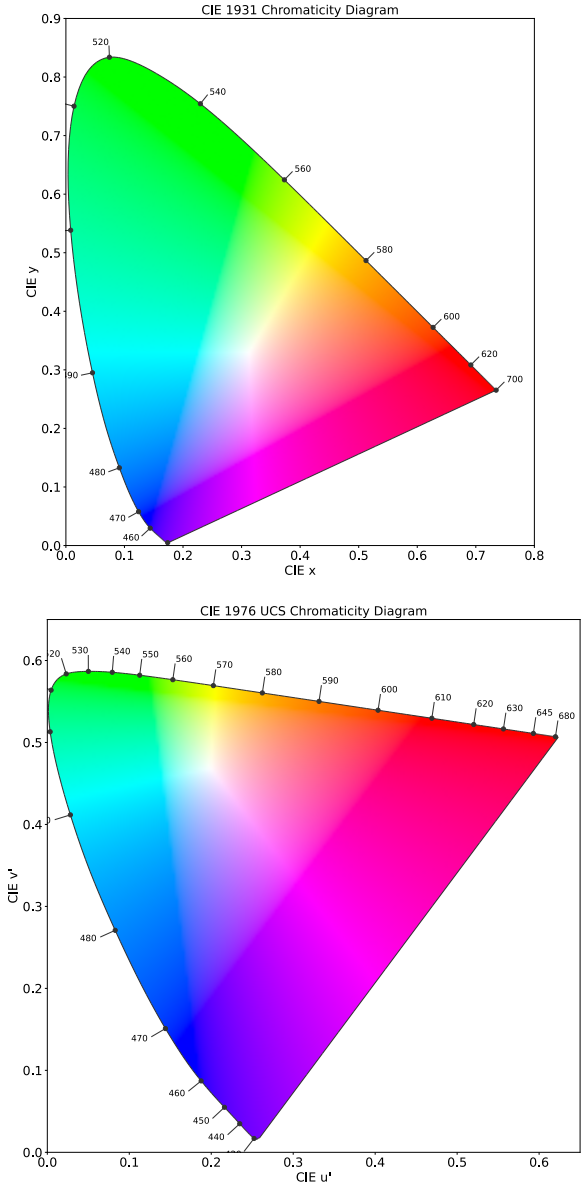

Figure 2.2: CIE 1931 xy and CIE 1976 u'v' diagram (Plotted using ColourPy).

CIELAB colour space

Though in many practical applications CIE xy and CIE u'v' chromaticity diagrams are sufficient for colour evaluation, it is crucial in some applications to not only assess chromaticity of a given colour sample, but also its lightness. This is why CIELAB (also CIE L*a*b*) colour space was invented. It is designed to be perceptually uniform, i.e. the Euclidean distance between any two colours in the space approximates the perceived difference between them. The CIELAB space is structured around three axes: L^*, a^*, and b^*, where the former one represents perceived lightness and the latter ones represent chromaticity coordinates (see Fig. 2.3) [5].

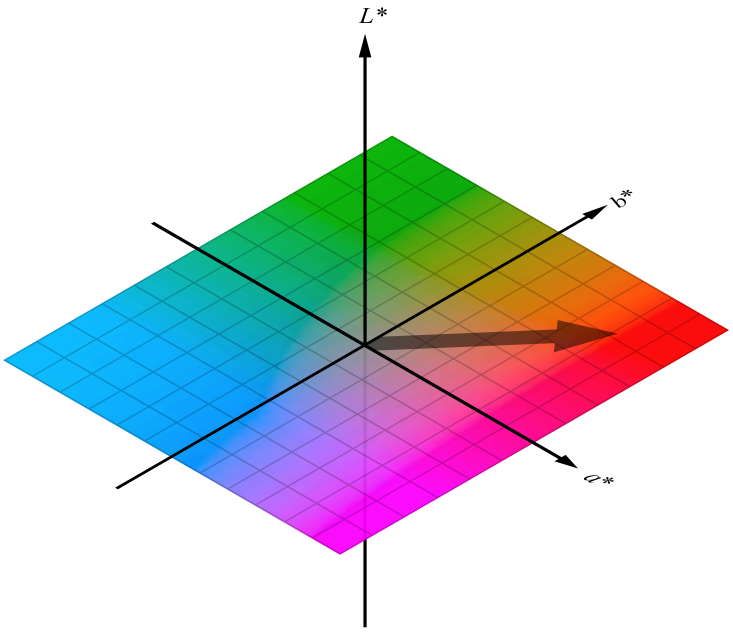

Figure 2.3: Example colour definition (by vector) in CIE Lab colour space (The image was taken from [8]).

L^* ranges from 0 (black) to 100 (white), whereas a extends from positive values for red/magenta to negative values for green, and b spans from positive values for yellow to negative values for blue. The relations between these parameters and the XYZ colour space are defined through non-linear transformations, that aim to mimic the non-linear response of the human eye to luminous intensity. These transformations involve intermediate variables, such as:

$$\begin{aligned} L^* &= 116 f(Y/Y_n) - 16, \\ a^* &= 500[f(X/X_n) - f(Y/Y_n)], \\ b^* &= 200[f(Y/Y_n) - f(Z/Z_n)], \end{aligned} \tag{2.2}$$

where X_n, Y_n, and Z_n are the XYZ tristimulus values of a specified white point, and $f(t)$ is a cube root-like function applied to each of X/X_n, Y/Y_n, and Z/Z_n [5].

The function may also be written in a non-linear form to match the human eye response:

$$f(t) = \begin{cases} t^{\frac{1}{3}}, & \text{if } t > \left(\frac{6}{29}\right)^3 \\ \frac{t}{3} \cdot \left(\frac{29}{6}\right)^2 + \frac{16}{116}, & \text{otherwise} \end{cases} . \tag{2.3}$$

As evident from (2.2) the HVS is able to perceive small differences in lightness levels more accurately at lower intensities (see Fig. 2.4).

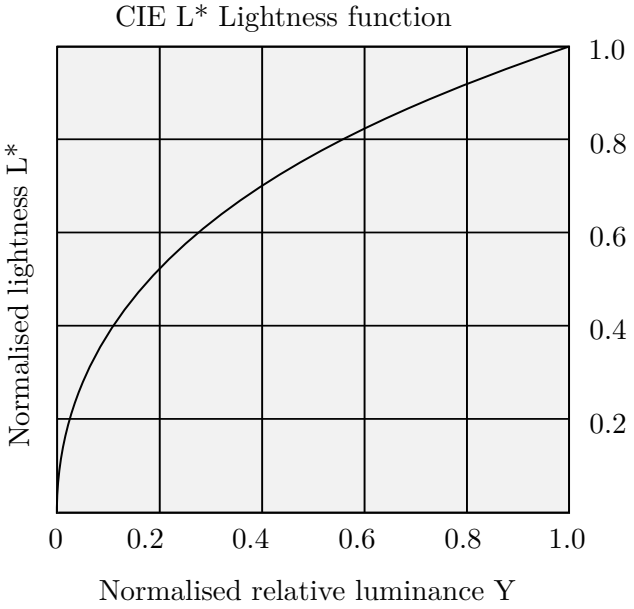

Figure 2.4: CIE L* lightness function in relation to the normalized CIE Y value (as per eq. 2.2, 2.3).

Display representation: RGB colour spaces and colour gamut

All the mentioned colour spaces intend to cover all the possible combinations of tristimulus values. Nevertheless there are of course physical restriction of how many colours can be displayed by modern displays. Thus a concept of some displayable colour set rises. This is what is called colour gamut. Color gamut is the complete subset of colours that can be accurately represented within a given colour space or by a specific display device. It defines the range of colours that a device (like a monitor, television, or printer) can display. Essentially, the gamut represents the palette of colours available to a device or in a colour model, which impacts how vivid and accurate the colour reproduction can be.

Most modern displays utilize gamuts grounded in RGB colour spaces – the ones that are defined by Red, Green and Blue primary colours (see Fig. 2.5).

RGB colour spaces are predominantly used in electronic displays such as computer monitors, televisions, and smartphones because they leverage light directly to produce colours. This model fits naturally with how such devices operate, using light-emitting diodes or liquid crystals that directly control the emission of red, green, and blue light [3, 22].

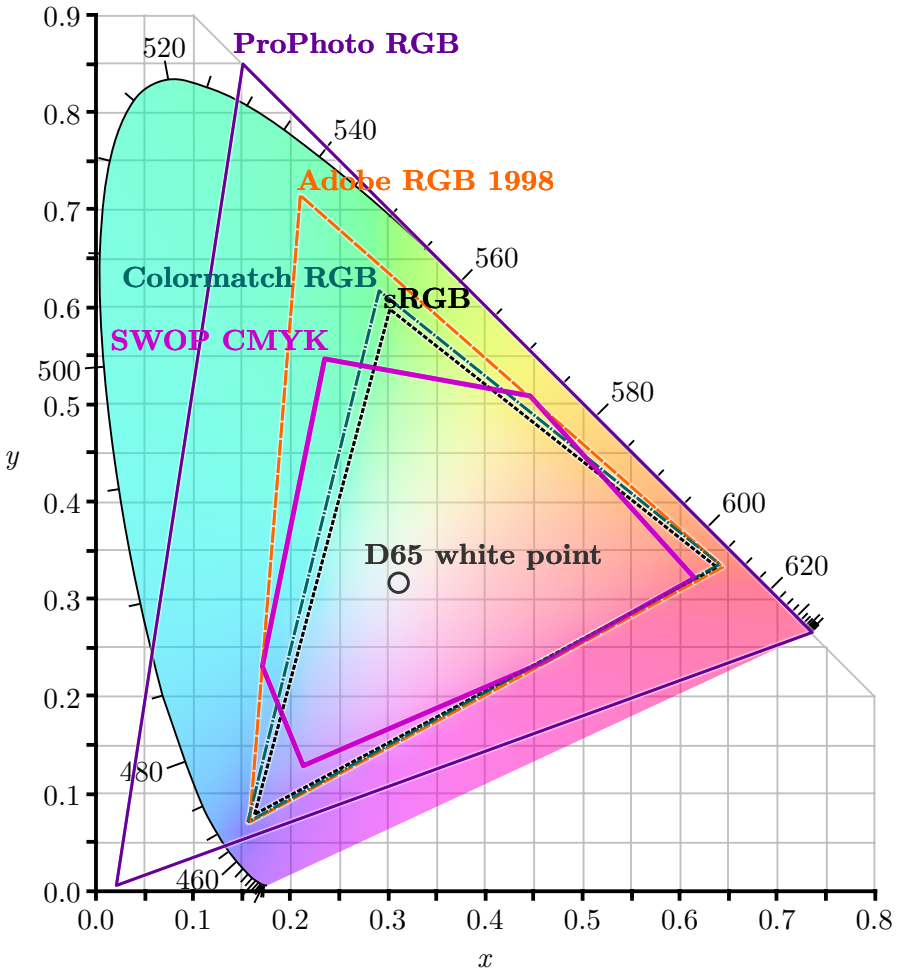

Figure 2.5: Comparison of different gamuts in relation to CIE 1931 xy chromaticity diagram (Taken from [7]).

2.2.2 Colour difference formulae

Having some colour strictly defined within some colour space brings us closer to colour difference perception testing. It is crucial though to firstly define colour difference inside the mentioned colour space itself. Color difference formulae allow for the quantification of the perceptual differences between two colours.

Most of CIE colour difference metrics, denoted ΔE^*, were originally designed to have the value of 1.0 to be equivalent for the smallest difference

perceptible by the HVS. These differences, called JND, will be more thoroughly discussed in this thesis further.

Initial CIE 1976 L*a*b* colour difference formula was grounded in the presumption of CIE L*a*b* uniformity. Thus this formula, commonly referred to as ΔE^*_{ab}, is calculated as follows:

$$\Delta E^*_{ab} = \sqrt{(\Delta L^*)^2 + (\Delta a^*)^2 + (\Delta b^*)^2}, \tag{2.4}$$

where ΔL^*, Δa^*, and Δb^* represent the differences in individual parameter of the colour space between two colours. For this particular formula JND is equal to 2.3 value [3].While this formula is an improvement over previous models, comprehensive tests prove that it still does not fully account for complete perceptual uniformity [18].

To address these and other shortcomings, the CIE refined the definition in 2000, resulting in the CIEDE2000 colour difference formula, which incorporates several adjustments to improve the assessment of colour differences, especially in regions where the CIELAB formula performed poorly:

$$\Delta E_{00} = \sqrt{\left(\frac{\Delta L'}{k_L S_L}\right)^2 + \left(\frac{\Delta C'}{k_C S_C}\right)^2 + \left(\frac{\Delta H'}{k_H S_H}\right)^2 + R_T \frac{\Delta C' \Delta H'}{k_C S_C k_H S_H}}. \tag{2.5}$$

The terms in the CIEDE2000 formula include:

- $\Delta L'$, $\Delta C'$, and $\Delta H'$ which are the differences in lightness, chroma, and hue (where chroma and hue are polar transformation of Cartesian chromaticity coordinates) modified to incorporate corrections for neutral colours (primed values indicating CIE94 modifications [3]);
- S_L, S_C, and S_H are scaling factors for lightness, chroma, and hue that compensate for the varying degrees of perceptual uniformity across these dimensions;
- R_T is a rotation function to account for the blue hue angle's problematic regions;
- k_L, k_C, and k_H are parametric factors to adjust the formula for different viewing conditions and applications [3].

As already mentioned above, the approximate value of almost every CIE metric is designed to be 1 for JND between two colours. Given the non-linearity of the formula, CIEDE2000 metric, as well as CIE94 metric, is very sensitive to the subtle changes, therefore when going slightly beyond the JND boundary the ΔE_{00} value significantly decreases. An illustrative example of this could be:

Coordinates	L^*	a^*	b^*
First colour	50	2.5	-0.5
Second colour	50	2.8	-0.2

The ΔE_{00} for these two colours is $\Delta E_{00} = 0.4748$, which is more than two times lower than the JND colour difference in the same metric.

2.2.3 Just noticeable difference and chromaticity discrimination ellipses

The Just Noticeable Difference (JND) in colour perception is defined as the smallest colour difference perceptible by the human eye under specific conditions. It considers the individual characteristics of the HVS, particularly its differential sensitivity to various colour channels. The JND can vary significantly across the RGB channels due to the HVS's varying sensitivity to different colours, allowing more changes to be tolerated in the red and blue channels than in the green.

Traditional colour difference formulae, while effective for many applications, exhibit limitations in predicting JND [34, 31]. To address this, chromaticity discrimination ellipses are constructed throughout the whole colour gamut as a tool to refine and better measure perceived colour differences.

Chromaticity discrimination ellipses were firstly described in the work of MacAdam, who first illustrated the non-uniformity of the CIE 1931 colour space through empirical measurements. These ellipses represent regions around a colour center within which colour variations are imperceptible to the average observer, essentially mapping out the just noticeable differences (JND) in colour perception [19].

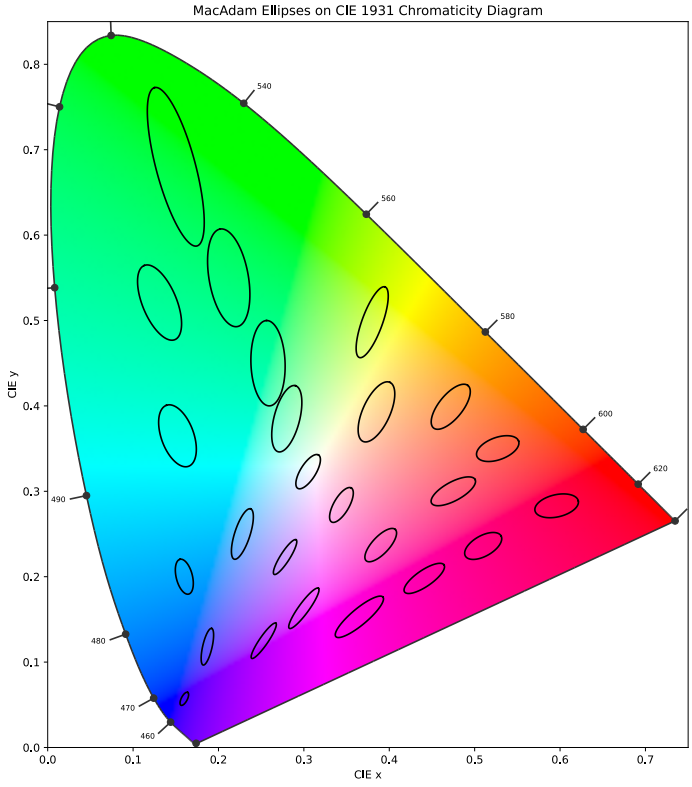

Figure 2.6: McAdam chromaticity discrimination ellipses as per his work [19] plotted in the CIE 1931 xy diagram. (Plotted using ColourPy; Data are taken from [33]; Ellipses are ten times enlarged).

One of the way of formulation of chromaticity discrimination ellipses in the CIELAB colour space, as introduced by the CIE, involves a quadratic equation with fitting constants g_{11}, g_{12}, and g_{22}, which are determined through psychophysical experiments involving colour matching assessments. The mathematical representation is given by:

$$g_{11}(\Delta a^*)^2 + 2g_{12}\Delta a^*\Delta b^* + g_{22}(\Delta b^*)^2 = 1, \tag{2.6}$$

where Δa^* and Δb^* denote the chromatic differences between the given colour and the colour center in the CIELAB space [31].

The significance of chromaticity discrimination ellipses extends beyond only illustrating the non-uniformity of colour spaces. They serve as a component in developing and evaluating colour difference metrics especially in high-quality display technologies. For instance, the exploration of ellipses in the context of wide colour gamut (WCG) displays revealed the limitations of existing colour difference formulae like CIEDE2000 in capturing variations in highly saturated colours [35].

2.3 Psychovisual experiments

This section aims to provide a state-of-art review in the field of psychovisual experiments and methods that are applied to acquire characteristics of HVS. Since the thesis's main topic is colourimetry this section will mainly discuss methods used for obtaining information about colour distinguishing abilities of one's HVS.

2.3.1 Assessment of colour differences

Modern studies of colour difference perception highly rely on chroma-independent techniques such as great-scale method [35, 34], which are usually applied for static colour evaluation.

Colour difference is measured for given colour centres, which are predefined reference points within a colour space, chosen to represent a wide spectrum of colours across the colour gamut. Colour difference pairs, consisting of a reference colour (from the colour centres set) and a comparison colour with slight variations, are used to measure perceptual colour differences. For that aim a grey-scale method can be used, as it is chroma-independent (all grey-scale samples have a^* and b^* set to zero).

The grey-scale method involves presenting observers with a series of grey scale pairs that vary in lightness, positioned adjacent to the colour difference pairs under examination. These grey pairs, chosen to cover a range of perceptual differences equivalent to those expected between the colour pairs, serve as a benchmark for comparison. Observers are tasked with estimating the colour difference of the test pair by selecting the grey scale pair that most closely matches this difference in terms of perceived lightness change (see Fig. 2.7). This comparative process enables the translation of colour differences into a quantifiable scale based on the grey scale pairs, thereby standardizing

the measurement of perceptual colour differences. The numerical value of the perceived difference (ΔV) is subsequently derived from the matched grey scale pair.

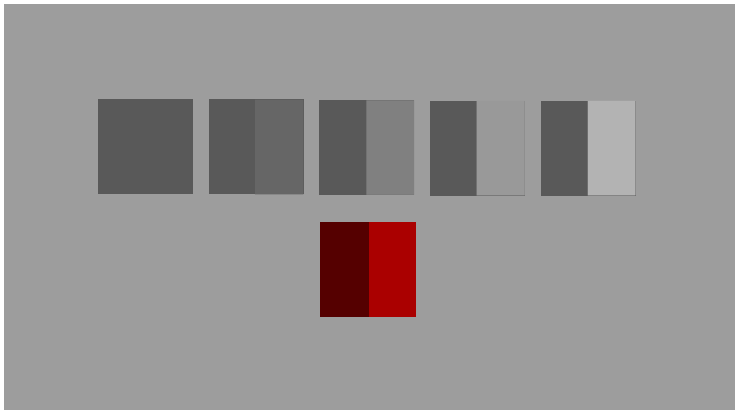

Figure 2.7: The principle of static colour difference evaluation using grey scale technique, where the expected colour differences of grey scale pairs (as per CIE colour difference formula) are known.

Quantifying colour difference: ΔV

The perceived colour difference, denoted as ΔV, is quantified through observer assessments against a standardized grey scale. This metric helps evaluating the performance of colour-difference models, it provides a numerical representation of visual perception [35]. The calculation of ΔV is expressed as:

$$\Delta V = k_1 \cdot e^{k_2 \cdot GS} - k_3, \tag{2.7}$$

where GS denotes the grey-scale value, correlating with the observers' judgement of colour difference magnitude and coefficients $k_1 - k_3$ are chosen to find the optimum of the following problem:

$$\{k_1, k_2, k_3\} = \arg \min_{\{k_1,k_2,k_3\} \in \mathbb{R}} |\Delta E^*_{ab,E} - GS|, \tag{2.8}$$

where $\Delta E^*_{ab,E}$ is experimental colour difference and GS are the preset grey-scale difference values used for the assessment [35, 17, 18]. The former is given by the formula already discussed in 2.2.2 (see eq. 2.4). The target function difference itself gives us predicted colour difference:

$$\Delta E^*_{ab,P} = \Delta E^*_{ab,E} - GS. \tag{2.9}$$

2.3.2 Evaluation of uniform colour spaces and colour difference formulae based on comprehensive visual datasets using proposed technique

The proposed technique could be utilized to both evaluate perception of colour difference in luminous and non-luminous modes (i.e. presenting colour

on monitor or as a printed sample) and allows for ensuing analysis of both uniform/non-uniform colour spaces fidelity and colour difference formulae validity based on retrieved results.

Comprehensive researches conducted by professor Luo et al. [34, 17, 18] may server as a very detailed reference and will be discussed in subsequent section.

The surface and luminous mode experiments were designed in [17, 35]. The surface mode experiment was conducted within a controlled dark environment using a spectrum-tunable LED viewing cabinet. This setup ensured consistent CIE D65 illumination (the most used standard illuminant, in other words standardised theoretical source of visible light with strictly defined colour temperature, which, in its turn, enables comparison of scenes, colours and images recorded under differing light conditions [3]) across nine distinct luminance phases. To quantify the perceived differences for all colour samples 6-level grey scale progression was used.

Luminous mode experiment utilized a calibrated NEC PA302W display, examining colour difference thresholds across six luminance levels. Luminous mode experiments presented in the papers always aimed to copy surface mode colour distribution. In all the luminous mode experiments spectroradiometer was used to ensure exact measurement of luminance and chromaticity parameters of the display.

After collecting data from observers the STRESS metric (see eq. 2.10) can be applied, which has proven to be very efficient for testing the performance of colour difference formulae, evaluating the difference between predicted and observed colour variance [34, 18, 17, 35, 21].

$$\text{STRESS} = \sqrt{\frac{\sum_{i=1}^{N}(f \cdot \Delta E_i - \Delta V_i)^2}{\sum_{i=1}^{N} \Delta V_i^2}}, \tag{2.10}$$

where

$$f = \frac{\sum_{i=1}^{N} \Delta E_i \cdot \Delta V_i}{\sum_{i=1}^{N} \Delta E_i^2} \tag{2.11}$$

is a scale factor adjusting recorded and expected (i.e. computed) colour difference to the same range.

Subsequently a statistical F-test was exploited to evaluate each of presented colour models' performance.

Based one the results of [34, 17, 18, 35] we can conclude that CIE models, such as CIEDE2000 (see eq. 2.5) and CIE 94, ranked second in evaluating both small and large colour differences being second only to CAM16-UCS colour space.

Commercial solutions for chromaticity discrimination

To analyze one's ability to discriminate between two colours for practical purposes (e.g. issuing driver licenses) commercial anomaloscopes are used. These are devices used to diagnose and analyze colour vision deficiencies,

particularly in the context of red-green colour blindness (dichromacy) and to quantify colour discrimination ability. An anomaloscope typically consists of a viewing apparatus where the subject looks into a pair of eyepieces. The device presents a test field composed of a mixture of red and green lights, which the subject adjusts to match a reference yellow light. By varying the proportions of red and green, the subject attempts to match the test field to the reference field [28].

2.3.3 Other HVS characteristics

Though this thesis mainly aims to discuss colourimetry parameters measurements of one's HVS, there are also several HVS characteristics that are bound with colour independent, or almost colour independent, mechanism of HVS. Here are a few examples of such.

2.3.4 Contrast Sensitivity Function (CSF)

The CSF is fundamental in measuring how sensitivity varies with spatial frequency, describing the lowest contrast that can be perceived at various spatial resolutions. This measure is crucial for understanding the visual system's capability in different lighting conditions and at varying distances.

Why Measure?

It was found that CSF plays a very vital role in the diagnosis of various neurodegenerative disorders like Parkinson's disease, Alzheimer's disease etc. Also it was concluded that it could be a relevant marker of incoming severe retinal disruption before pathological problems occur, establishing that, for instance, CSF is an important marker to evaluate glaucoma patients' ability to undertake daily life tasks [26, 4, 25].

How to Measure?

CSF measurement is typically achieved through psychophysical tests using sinusoidal gratings that vary in frequency and contrast or some other patterns with the same altering parameters. Two primitive methods for CSF measurement include the Arden gratings test and the Pelli-Robson chart (see Fig. 2.8).

The Pelli-Robson chart is used to measure contrast sensitivity by assessing the ability to read large letters that gradually decrease in contrast. The chart consists of rows of letters grouped in triplets, with each triplet having the same level of contrast. The patient reads the letters aloud from a specified distance, typically 1 meter, starting with the highest contrast at the top. The lowest contrast level at which the patient can correctly identify at least two letters in a triplet determines their contrast sensitivity score [23].

The Arden gratings test measures contrast sensitivity using striped patterns (gratings) that vary in contrast and spatial frequency. The patient views

these gratings on a screen or chart, which are presented at different contrasts and frequencies. The patient is asked to identify the orientation or presence of the gratings. The results are plotted on a graph, with contrast sensitivity on the vertical axis and spatial frequency on the horizontal axis, creating a contrast sensitivity function (CSF) that profiles the patient's ability to detect contrast at different spatial frequencies [30, 1].

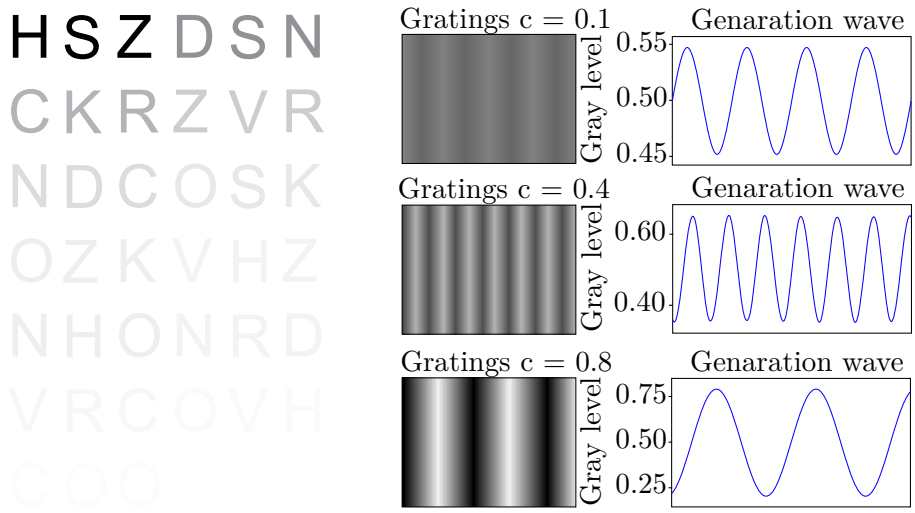

Figure 2.8: The Pelli-Robson chart (on the left) and the Arden gratings test generated for three different contrast and spatial frequency levels (on the right).

2.3.5 Visual acuity

Visual acuity is the clarity or sharpness of vision. It measures the ability of the eye to discern shapes and the details of objects at a specific distance, usually standardized, for instance at 20 feet [6, 32].

Why Measure?

Visual acuity measurement is a basic procedure in the detection and follow-up of healthy vision. It helps identify vision problems—nearsightedness, farsightedness, or such conditions that may be corrected by glasses or surgery—and also demonstrates changes in vision over time, thus leading to appropriate treatment and intervention.

How to Measure?

The most basic instrument for conducting a measurement of visual acuity almost everyone is acquainted with is Snellen chart, invented in the late eighteen hundreds yet still widely used among ophthalmologists (see Fig. 2.9).

The task for the individual is to identify the smallest size they can read in the chart, which uses fractions to measure visual acuity: the numerator

represents the distance of the subject from the chart, typically 6 meters or 20 feet. The denominator indicates the distance at which a person with standard vision could read the same line. For example, a 20/20 vision means the line can be read by a typical person at 20 feet. Conversely, the notation 20/200 suggests that a line readable at 200 feet by someone with normal vision could only be read at 20 feet by the observer [6].

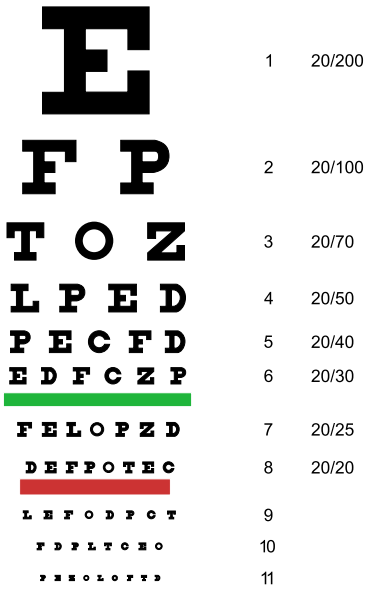

Figure 2.9: Schematic depiction of Snellen chart [11].

Chapter 3

Realization of a tool for colourimetric psychovisual experiment

This part describes the empirical side of the study in which a tool was designed that allows, by mean of psychovisual experiment, for evaluation of colourimetric parameters of the presented colours and human visual system's response to them. The uniqueness of the tool lies in it's ability to measure across the area of the specified gamut and to automatically reevaluate multiple colourimetric parameters of the presented colour samples after the test to provide maximum precision. Firstly, we are going to describe the instrument and it's program's flow.

3.1 General description

The first part of the thesis has shown that most of the studies utilized static methods of colour assessment, i.e. non-changeable colour pairs difference is being evaluated using reference grey-scale colour pairs (see Fig. 2.7). In this thesis's experimental part we intended to apply dynamic evaluation method and compare the results obtained by utilizing it with the ones achieved when using static methods (2.3.2).

Our aim was to devise, given the certain equipment and environment (see 4.1), an instrument that would permit the evaluation of the HVS's colour distinguishing capabilities and at the same time would return lucid visual outputs and a vast spectrum of parametric information on presented colour samples. The proposed tool is comprised of several scripts devised to conduct a psychovisual experiment in the form of colour matching test and then to present the results of the testing in a lucid form.

3.1.1 Psychovisual experiment tool

At the experiment initialization the program asks the observer to fill in their personal data, i.e. age, gender, name and general remarks (such as visual disorders, psychological condition etc.) as well as the complexity of the test designated with the number of directions in which each of presented colour centres are to be approached (we will describe the testing concept

more thoroughly in the following sections).

After the data acquisition the observer proceeds to the colour picking menu, where three options are at the disposal:

1. To use a colour picker tool, which would return chosen colours' L^* a^* b^* coordinates. The L^* lightness level can be set manually in the code (50 is default);
2. To use colours preset defined in a CSV table of the same name;
3. To use the colours from the latest test.

After the colour picking process an observer is asked to either proceed to colour fidelity test, which is designed to let the subject manual measurement of all the colour samples, i.e. both colour centers and the points that are to be adjusted to match them, assuring that every piece of visual information used in the testing is presented correctly on the screen (see Fig. 3.1), or proceed to the testing itself. Here follows its description.

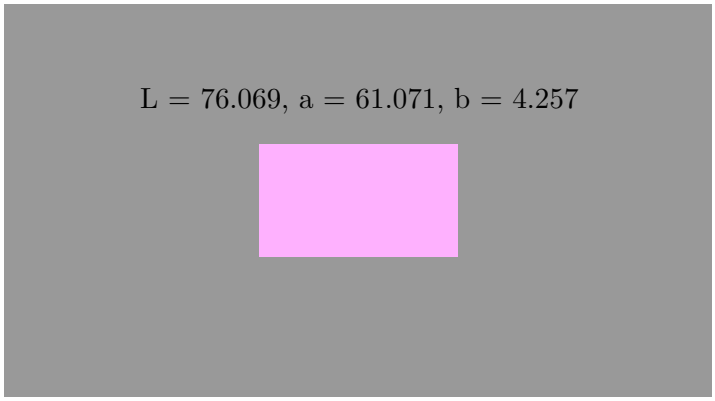

Figure 3.1: Colour fidelity test environment for optional manual measurement of the samples to be used in the testing.

3.1.2 Colour matching test

After proceeding to the test each subject is at first shown a seamless gray-scale sample sized to match the full screen. This demo lasts for five seconds to let the subject's HVS accommodate to the luminance conditions of the set-up. During all the phases of the pilot experiment discussed further in the thesis the adaptation sample's configuration remained unchanged across all the observers to ensure that no chromaticity shift is caused by the difference in the luminance adaptation conditions [20]. The parameters of the adaptation sample are recorded in Tab. 3.1.

Colour matching test in its essence is a sequence of colour pairs presented to an observer in a form of adjacent equally sized squares where the left sample is chromatically fixed, i.e. colour centre, whereas the right sample is the one the observer is asked to adjust along multiple fixed axes in the CIE

Type of parameters	L^*	a^*	b^*
Passed in parameters	50	0	0
Measured parameters	48.79	-2.02	0.07

Table 3.1: Adaptation gray-scale sample parameters including actual physically attained parameters measured using JETI Spectroval 1511 HiRes rounded to 2 decimal points.

a^*b^* plane using keyboard (specifically keys: ← and →) until no difference is evident (see Fig. 3.2). The number of fixed axes is set, as mentioned above, at the data acquisition stage.

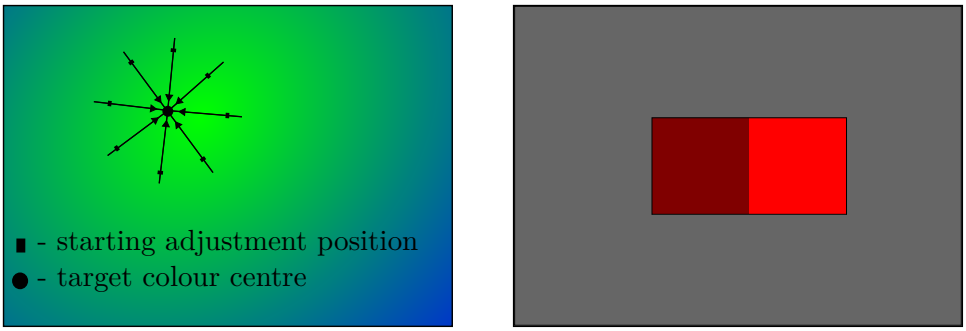

a) b)

Figure 3.2: a) Schematic explanation of how central colour is approached in CIE a^*b^* chromaticity plane from starting points; b) Visual interface of the testing environment with the left sample representing fixed colour centre and the right colour representing dynamically adjusted sample.

After matching the fixed colour N times (where N denotes the number of directions), i.e. approaching the colour from different generated positions in the CIE a^*b^* plane, and acquiring data of colours which are perceptually indistinguishable from the center observer proceeds to the next examined fixed colour and the cycle repeats.

An example output table for one observer testing 2 colours in 8 directions is presented in the Tab. 3.2:

Name	Gender	Age	Test	General rem.	Adj. L^*	Adj. a^*	Adj. b^*
Václav	Male	25	1	None	L	a_{11}	b_{11}
Václav	Male	25	1	None	L	a_{12}	b_{12}
...	...	...	...	...	...	...	...
Václav	Male	25	2	None	L	a_{27}	b_{27}
Václav	Male	25	2	None	L	a_{28}	b_{28}

Table 3.2: An example output of the colour matching test for an observer testing two colour centres in eight directions.

Where Test designates tested colour center index and $a_{ij}b_{ij}$ stands for the parameters of the j-th adjusted, perceptually indistinguishable colour sample

laying near i-th colour center.

When all the colour difference pairs in the set are matched two options are proposed: either to proceed to the next observer or finish the evaluation. The results are saved in the CSV format in the 'results' directory (for more transparent data management structure see Fig. 3.3).

In case the 'Proceed to the next observer' option is chosen, the same data set is tested on the next subject after their personal information is acquired. To achieve high interobserver reliability of the resulting data, directions in which the target colour is approached are randomly shuffled (e.g.: the 8 directions order for one observer might be 0°-45°-90°-...-315° while for the other it might be 45°-225°-0°... etc.).

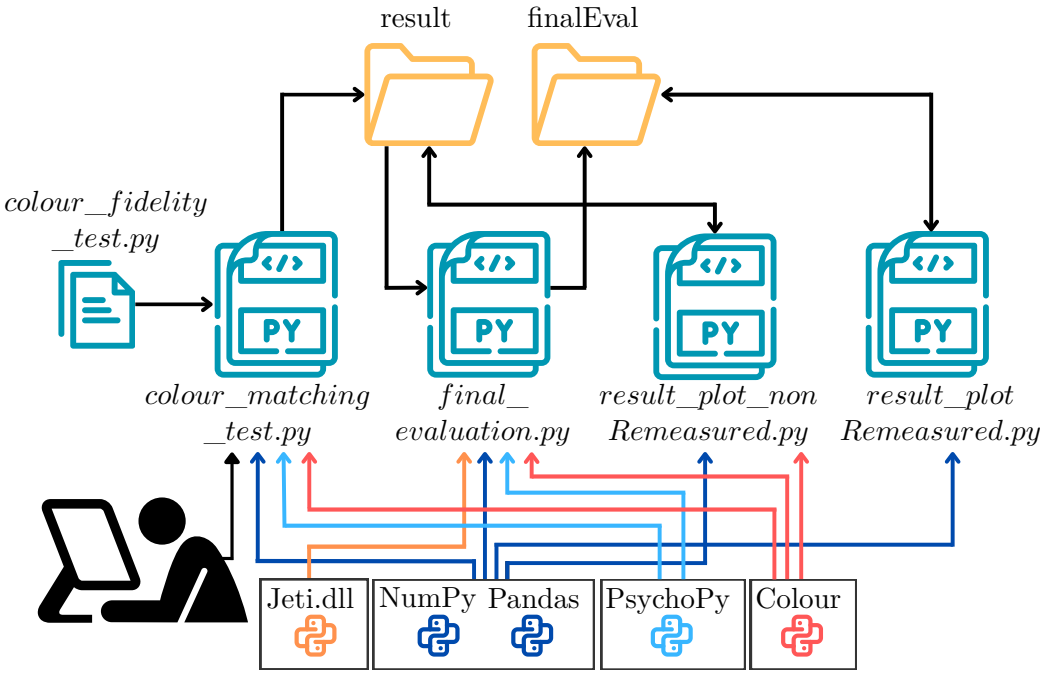

Figure 3.3: Program data management and file distribution scheme.

3.1.3 Reassessment option

Since we cannot rely solely on automatic display calibration during the experiment (see [10], Fig. 3.4), a script is proposed as a part of the designed tool to provide an option of verifying the obtained values by automatically measuring all the presented colours using the JETI Spectroval 1511 HiRes spectroradiometer [14].

After running the *final_evaluation* script, all the colours used during the experiment, including both the colour centers and the data marked by subjects as indistinguishable from them, are automatically sequentially displayed on the screen and measured by the spectroradiometer (see Fig. 3.5, 3.4).

The output of the program is a CSV table containing the following parameters for each sample: CIE XYZ tristimulus values, coordinates in the CIE

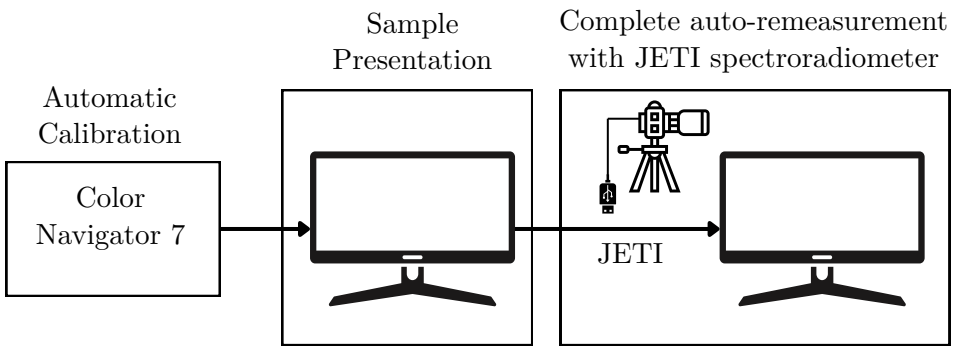

Figure 3.4: Schematic principle of the double colour fidelity verification implemented in the tool with the use of automatic calibration of the EIZO CG318-4K [10] and the JETI Spectraval 1511 HiRes spectroradiometer.

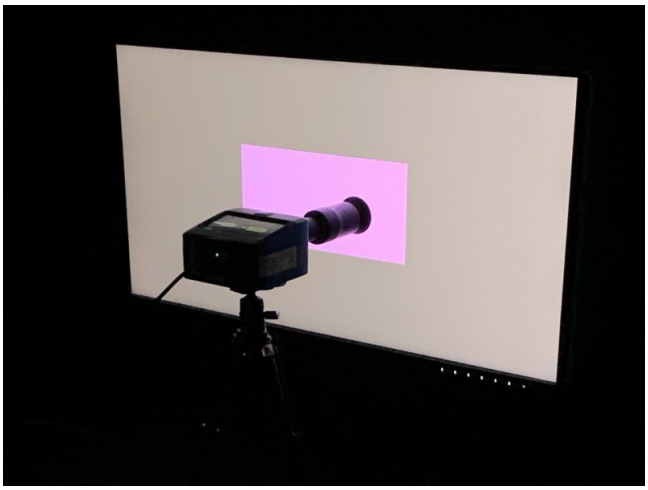

Figure 3.5: Set-up for automatic observer input reassessment using JETI Spectraval 1511 HiRes.

xy (CIE 1931 colour space) and CIE 1976 u'v' (CIE 1976 UCS) diagrams, as well as spectral intensities for each wavelength within the visible spectrum (380 – 780 nm) in 1 nm increments. The table is saved in 'finalEval' directory (see Fig. 3.3).

3.1.4 Plotting the results

After obtaining the results – either from the observers or both from the observers and the reevaluation mechanism – there is an option to visualize them. For both types of data multiple choices are provided:

1. To plot only the colour centres and the points marked as indistinguishable;
2. To plot only chromaticity discrimination ellipses;
3. To plot both.

Chromaticity discrimination ellipses' parameters are defined to solve the least squares task for individual colour centres' data sets:

$$(a_i, b_i, \theta_i) = \arg \min_{(a_i, b_i, \theta_i)} \sum_{j}^{K} d_{ij}, \tag{3.1}$$

where a_i, b_i, θ_i denote major axis, minor axis and rotation angle of the major axis of the i-th ellipse respectively and d_{ij} denotes the distance of the j-th point related to the i-th ellipse from this ellipse.

To avoid distortion of the ellipse by outlying points – which may occur due to erroneous inputs by some participants during the test (e.g. untimely key presses) – the points is filtered before the fitting using a z-score [24] (see eq. 3.2) with a threshold of $z = 2.5$

$$z = \frac{x - \mu}{\sigma}, \tag{3.2}$$

where μ and σ are the mean and the standard deviation of the population respecitvely.

Chapter 4

Pilot experiment

This chapter introduces the pilot experiment conducted for the tool's performance demonstration.

4.1 Experiment setup

The experiment was conducted in a darkened room. An EIZO CG318-4K monitor in an 8-bit configuration (8 bits per colour channel) with inbuilt calibration sensor was utilized for displaying colours and thereafter a JETI Spectraval 1511 HiRes was employed to remeasure all the acquired data to make sure the observers were presented correct colours (for key spectroradiometer's and monitor's characteristics see Appendix A). The performance of the tool can be increased by using 10 bpc regime, which is suggested for the future work with the program. The 8 bpc regime was used, even though the monitor allowed for 10 bpc, due to the restrictions of the graphics card.

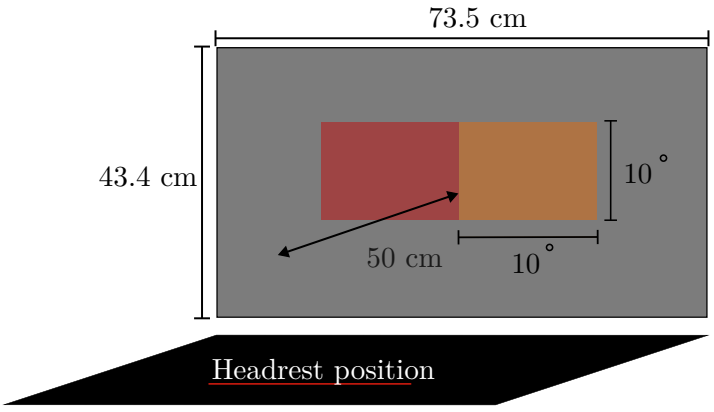

Figure 4.1: Scheme of the experimental setup configuration with designated monitor distance, visual angle and the dimensions of the monitor.

During the test each observer's head was placed in a headrest within 50 cm distance from the screen to preserve stable measurement conditions and guarantee interobserver reliability of the results. Given this stable viewing distance the displaying software – PsychoPy (see Fig. 3.3) – was manually set during the experiment to the visual angle mode, which allowed for presenting

the samples under an angle of 10°. In total ten people partook in the experiment.

4.1.1 Monitor performance

The monitor was at first calibrated using ColorNavigator 7 software distributed by EIZO [10].

For the test's comprehensiveness ITU-R Recommendation BT.2020 gamut was utilized. As a consequence of physical restrictions the monitor could not represent the whole gamut properly (especially given the fact it is initially designed to be exploited in DCI-P3 gamut). Taking this fact into consideration we have measured all the primary colours and the white points of the mentioned ITU-R Recommendation BT.2020 along with DCI-P3 and sRGB gamuts using previously mentioned JETI Spectraval 1511 HiRes. Obtained results are presented in Fig. 4.2.

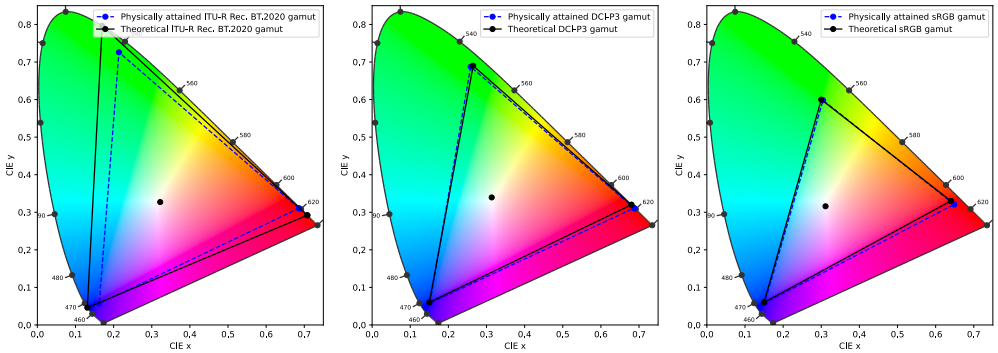

Figure 4.2: Theoretical gamuts' parameters of the EIZO CG318-4K monitor plotted out with the physically attainable values of the primaries and the white points of individual gamuts.

The physically attainable ITU-R Recommendation BT.2020 gamut was considered when picking the colour centres for the preset used in the pilot experiment (see Apendices). The percentage of cover resulted from our measurement (see Fig. 4.2) is 79.57% and the percent declared by the manufacturer is 80% [9].

4.2 Experiment: Phase 1

In the first phase of the experiment a preset of colours was tested. The designed environment allows to choose tested colour or set of colours using in-built colour picker, nevertheless the subjects were presented a predefined set of colours to more systematically cover the utilized REC2020 RGB colour gamut and analyze HVS response under the widest conditions scale possible to more thoroughly assess HVS capabilities regarding colour distinguishing. The predefined set is presented in Tab. 4.1.

#	L^*	a^*	b^*
1	76.069	-65.162	62.132
2	76.069	4.757	58.180
3	76.069	69.438	55.038
4	76.069	61.071	4.257
5	76.069	53.855	-62.270
6	76.069	-40.946	28.360
7	76.069	-5.928	-14.477
8	76.069	24.164	35.191

Table 4.1: CIE L*a*b* coordinates of the predefined tested colours used in the first and the second phase of the pilot experiment.

It is also important to mention that when picking colour centres we payed attention to the fact that there had to be some reserve between the samples and the borders of the gamut to avoid misrepresentation (see Fig. 4.3).

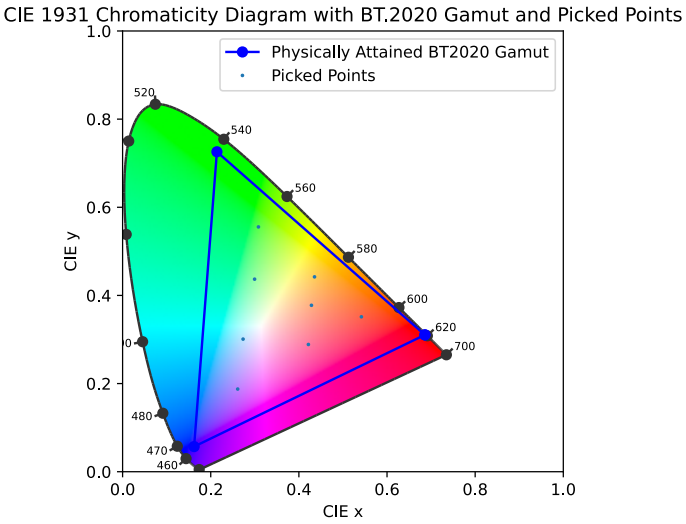

Figure 4.3: Colour centres from the predefined set 4.1 picked to systematically cover the utilized ITU-R BT.2020.

The preset was generated using colour picker that considered the real monitor luminance performance and converted the CIE xy coordinates into the CIE L*a*b* using xyY to $L^*a^*b^*$ conversion, where the Y value was set to 50 to provide a balanced luminance setting across all colour samples and ensure that the initial luminance parameter for all the tested colours lays in the photopic region (see 2.1.1). This value was also chosen to approximately match the conditions of the McAdam's work, who has used the value of $L = 48$ cd/mm^2 [19] (for the utilized colour picker interface see Appendix C).

To achieve data comprehensiveness while preserving its compactness and ensuring the final evaluation does not last too long the $N_{\text{directions}}$ was set to ten in the first two phases of the experiment.

At this phase of the testing the monitor was calibrated on 100 cd/m^2 luminance. The results are presented below:

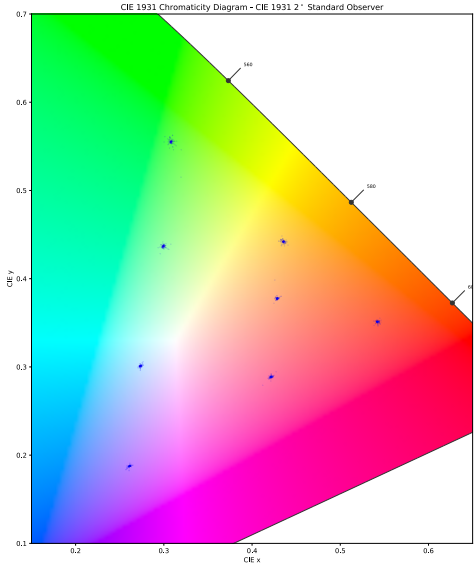

Figure 4.4: Values obtained in the first phase of the experiment for the monitor calibrated on 100 cd/m^2 luminance level; Plotted in CIE 1931 xy diagram.

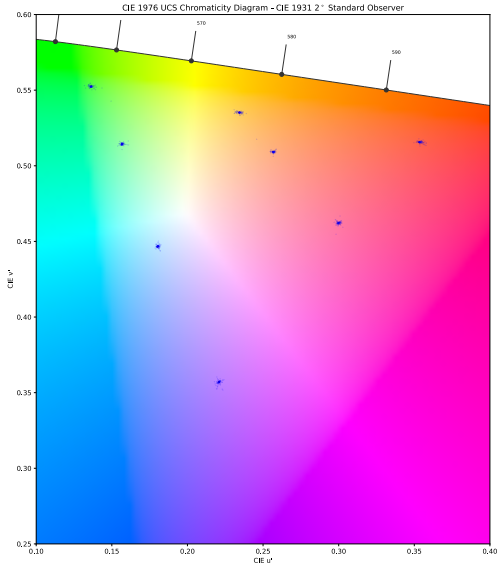

Figure 4.5: Values obtained in the first phase of the experiment for the monitor calibrated on 100 cd/m^2 luminance level; Plotted in CIE 1976 u'v' diagram.

In the figures 4.4 and 4.5 we may see the colour centres defined in the preset (see Tab. 4.1) marked as red crosses and the points chosen by the observers as indistinguishable from the mentioned centres marked as blue circles.

Here follow the diagrams depicting the real, physically attained values, remeasured by JETI Spectraval:

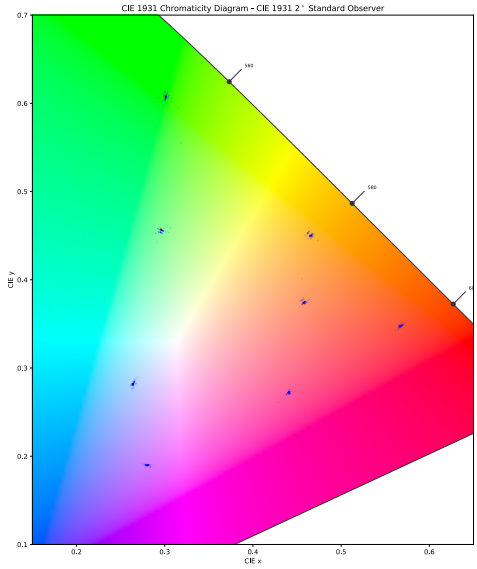

Figure 4.6: Remeasured values from the first phase of the experiment 4.4; Plotted in the CIE 1931 xy diagram.

In this diagram a distortion in relation to Fig. 4.4 is evident in the green and violet area, which have already proven to be more unstable regions of the utilized ITU-R Reccomendation BT.2020 gamut (see Fig. 4.2).

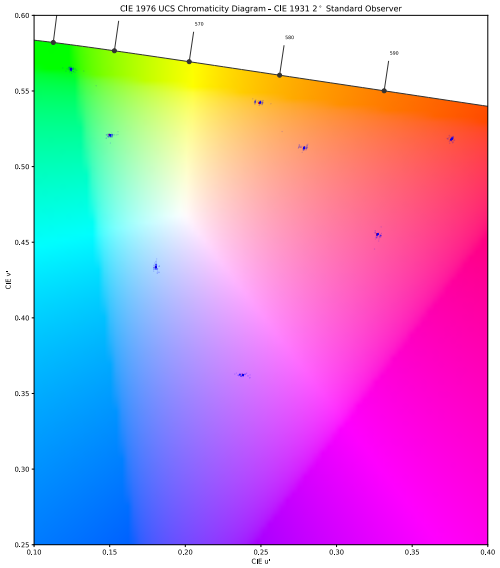

Figure 4.7: Remeasured values from the first phase of the experiment 4.5; Plotted in the CIE 1976 u'v' diagram.

The same trend as in the Fig. 4.6 is subsequently preserved in the CIE u'v' diagram (see Fig. 4.7).

For the clear arrangement of the visual data we will only enclose fitted ellipses without the points used for the fit (only the first and the second option from 3 are used in the main part of the thesis). For more thorough assessment of the experiment's results you can find the ellipses plot along with the points in the Appendix C.

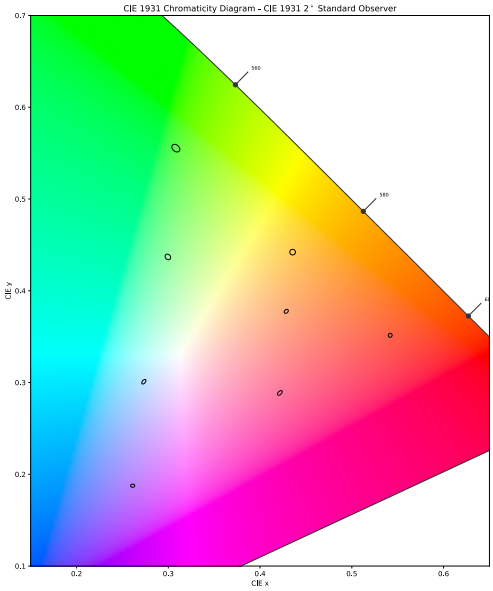

Figure 4.8: Ellipses fitted on the data before their remeasurement 4.4; Plotted in the CIE 1931 xy diagram.

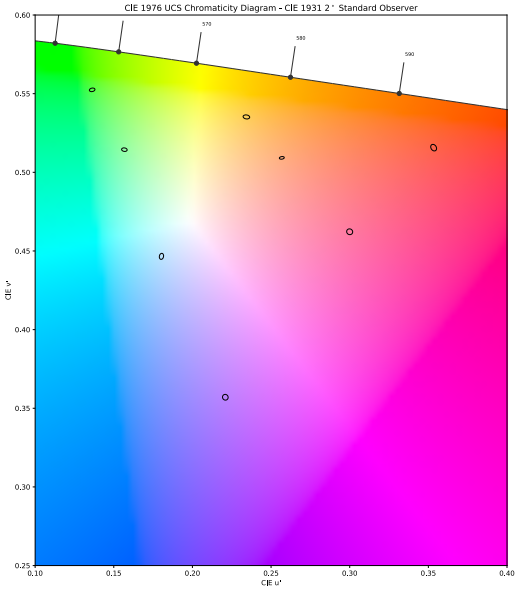

Figure 4.9: Ellipses fitted on the data before their remeasurement 4.5; Plotted in the CIE 1976 u'v' diagram.

Fitted ellipses (see Fig. 4.8, 4.9) bear a resemblance to the kind of the ones that were obtained by McAdam in his work [19]. The difference is though evident in their size, which is obviously a result of the higher luminance level maintaned in this phase of the experiment. The last step of the results evaluation in this phase would be plotting of the ellipses fitted on the data remeasured by the spectroradiometer (see Fig. 4.6 and Fig. 4.7):

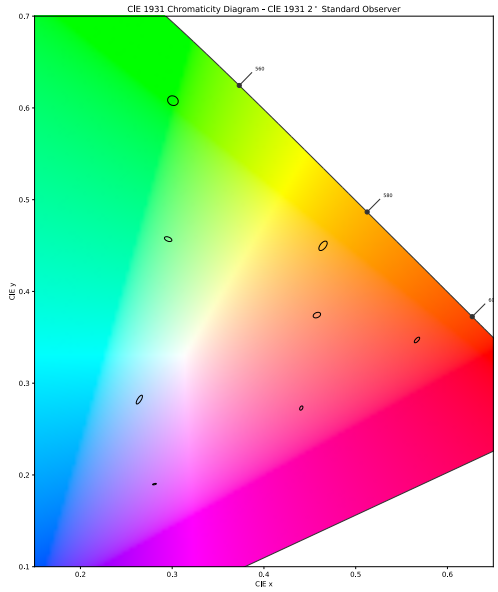

Figure 4.10: Ellipses fitted on the data subjected to the reevaluation using JETI Spectraval 1511 HiRes 4.6; Plotted in the CIE 1931 xy diagram.

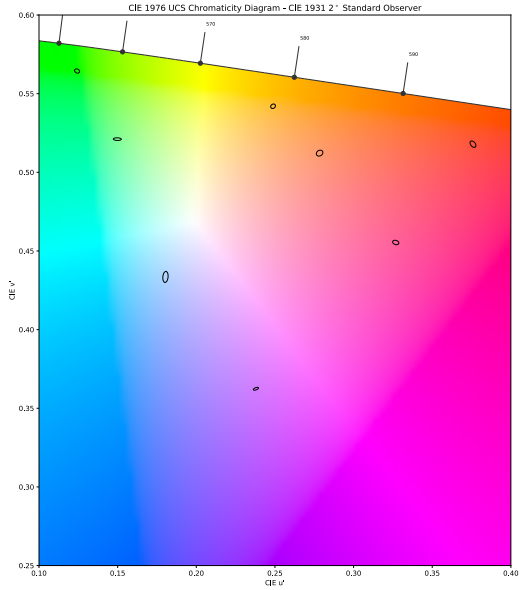

Figure 4.11: Ellipses fitted on the data subjected to the reevaluation using JETI Spectraval 1511 HiResv 4.7; Plotted in the CIE 1976 u'v' diagram.

The ellipses fitted using reevaluated data (see Fig. 4.10, 4.11) preserved the general structure present in the ones that were fitted relying solely on the display auto-calibration (see Fig. 4.8, 4.9) which advocates for the program's relatively stable performance with the given set-up in the high luminance (photopic) conditions. To compare the model to the existing models, we have computed the mean and the median colour differences in accordance with CIEDE2000 (see Eq. 2.5) and CIE94 colour difference formulae:

Colour center number	Mean ΔE_{94}	Median ΔE_{94}	Mean ΔE_{00}	Median ΔE_{00}
1	0.389	0.261	0.344	0.227
2	0.468	0.367	0.547	0.367
3	0.325	0.263	0.365	0.285
4 (Cherry)	0.316	0.183	0.278	0.157
5 (Violet)	0.263	0.129	0.245	0.119
6	0.435	0.281	0.390	0.263
7 (Green)	0.512	0.417	0.612	0.451
8 (Red)	0.429	0.267	0.486	0.305

Table 4.2: The mean and the median ΔE_{00}, ΔE_{94} values of the indistinguishable points obtained during the experiment, phase 1.

The values in the Tab. 4.2 exhibit the nature corresponding with the findings established in the theoretical part of the experiment, i.e. bigger colour difference between two colours, one of which lays close to the JND boundary of another is observed in the chromatically-saturated area (samples 7 and 8) , whilst lesser difference is evident in the 'violet' regions (samples 4-5).

The parameters of the physically attained colour centres displayed during the first phase of the test are presented the Tab. 4.3:

#	L^*	a^*	b^*
1	72.774	-64.097	59.122
2	71.213	3.998	54.200
3	72.502	66.231	57.415
4	73.811	61.124	4.881
5	72.299	56.005	-59.907
6	71.064	-38.744	26.500
7	70.927	-6.141	-14.719
8	72.191	21.806	36.200

Table 4.3: CIE L*a*b* coordinates of the predefined tested colours 4.1 subject to remeasurement using JETI Spectraval.

Values stated in the Tab. 4.3 correspond with the measuring specifications of the spectroradiometer (see Appendix A) and, along with the visual outputs,

prove the stability and precision of the implemented instrument in the photopic range. To maintain purity of the text we will further also enclose only the remeasured values of colour centres, not all the samples used during the test.

4.3 Experiment: Phase 2

In the second phase of the experiment the same preset of data was tested on the same group of observers. The only change was in the monitor's luminance calibration level, which now was set to 40 cd/m^2. Thus the luminance level was shifted towards lower values yet still of course remained in the photopic visual range [29].

In the figures 4.12 and 4.13 the results of the colour matching experiment for 40 cd/m^2 luminance level of the same colour samples as in the Phase 1 (see Tab. 4.1) are presented.

From these results it is evident that on average with the reduction of luminance an observer tends to evaluate more distant samples as indistinguishable. The main trends of the experiment results – i.e. points distribution – much resemble the ones observed in the first phase (see 4.2).

The results are presented below:

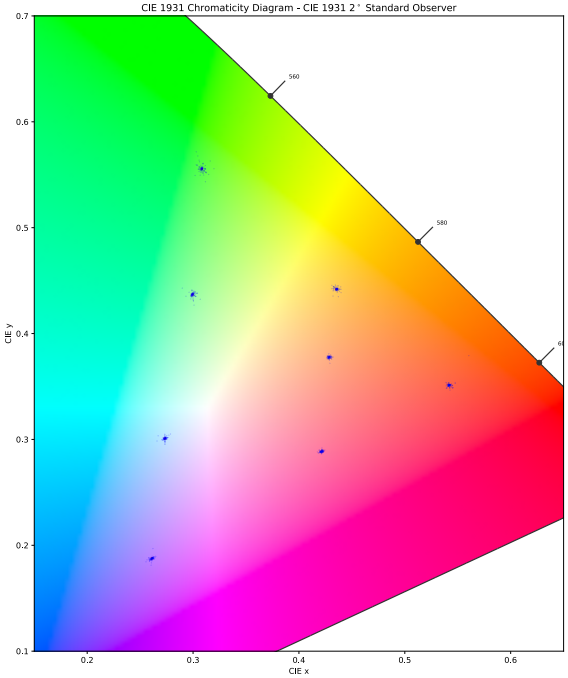

Figure 4.12: Values obtained in the second phase of the experiment for the monitor calibrated on 40 cd/m^2 luminance level; Plotted in CIE 1931 xy diagram.

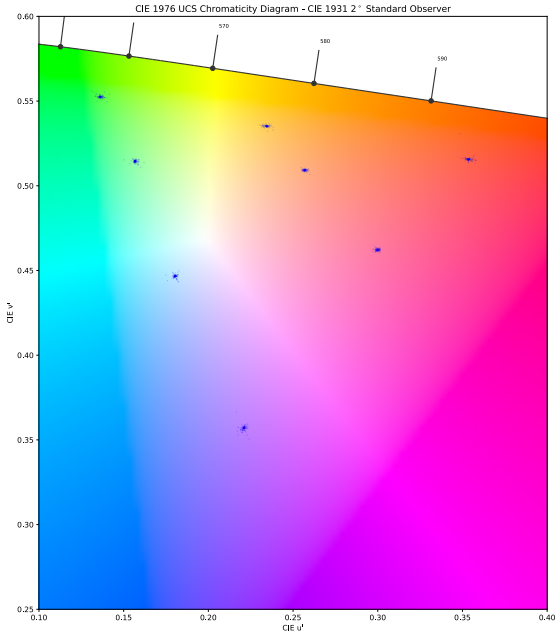

Figure 4.13: Values obtained in the second phase of the experiment for the monitor calibrated on 40 cd/m^2 luminance level; Plotted in CIE 1976 u'v' diagram.

Here follow the diagrams depicting the real, physically attained under the second phase's conditions values, remeasured by JETI Spectraval (see Fig. 4.14, Fig. 4.15):

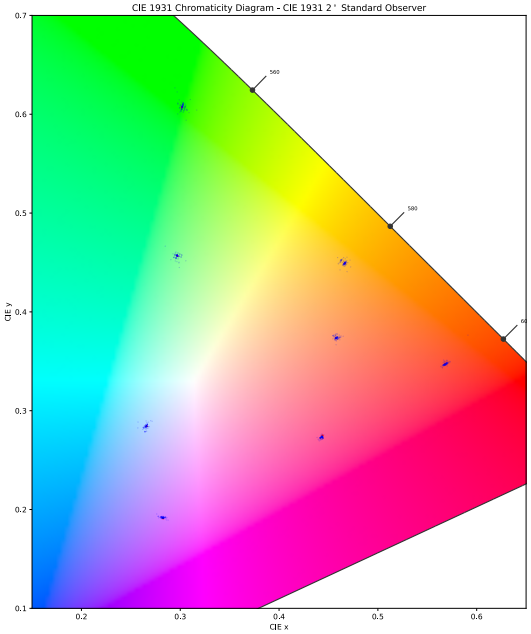

Figure 4.14: Remeasured values from the second phase of the experiment 4.12; Plotted in the CIE 1931 xy diagram.

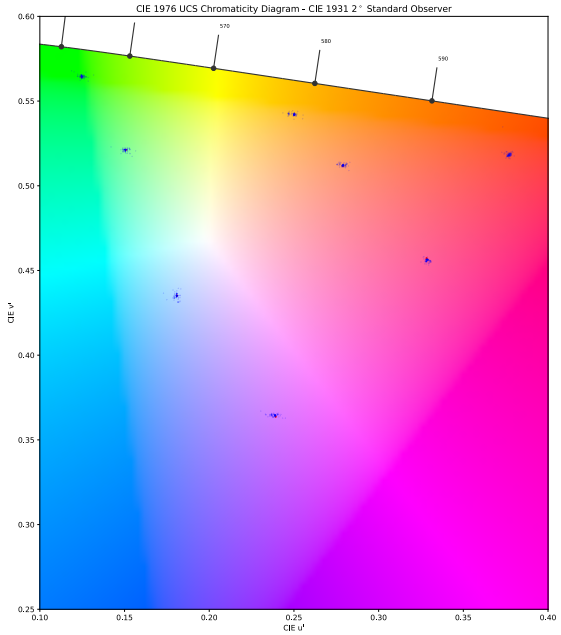

Figure 4.15: Remeasured values from the second phase of the experiment 4.13; Plotted in the CIE 1976 u'v' diagram.

Slight data distortion is observed in Fig. 4.14 and Fig. 4.15 in the blue-violet and the green area, though in general the data distribution preserves in relation to the one introduced above (see Fig. 4.12 and Fig. 4.13).

Here we once again (as well as in the Phase 1 4.2) introduce the results in the form of chromaticity discrimination ellipses:

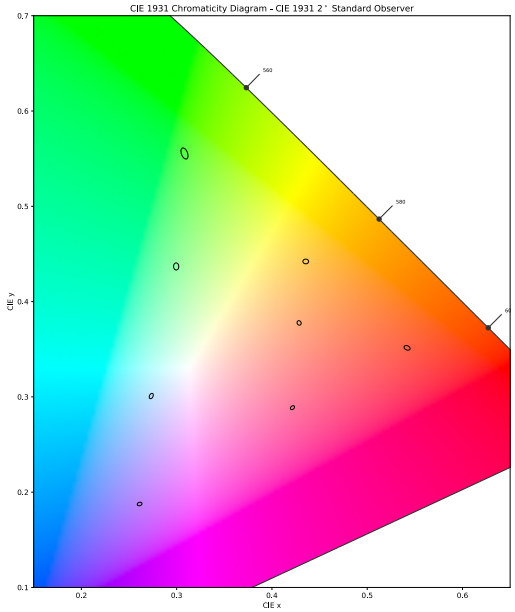

Figure 4.16: Ellipses fitted on the data before their remeasurement 4.12; Plotted in the CIE 1931 xy diagram.

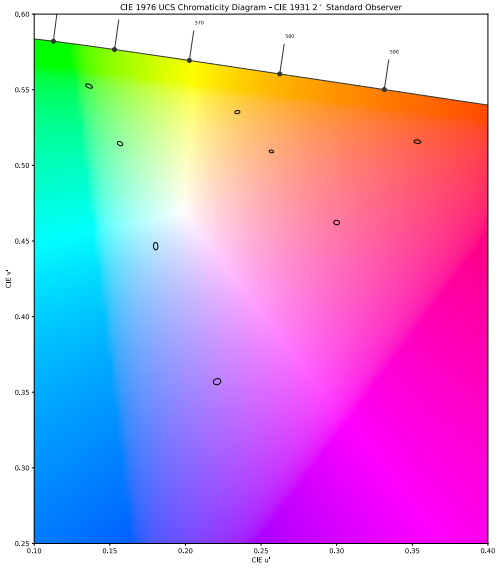

Figure 4.17: Ellipses fitted on the data before their remeasurement 4.13; Plotted in the CIE 1976 u'v' diagram.

Fitted ellipses in general preserve the shape and the rotation of the ones obtained in the first phase of the experiment with that little difference, that the ellipses in the second phase are perceptually slightly bigger, which corresponds to the way, in which the points distribution in the Fig. 4.14 and Fig. 4.15 differed from the ones in the first phase. (See Fig. 4.6, Fig. 4.7).

Here we also – as introduced in the first phase – enclose the ellipses fitted on the remeasured data (see Fig. 4.14 and Fig. 4.15):

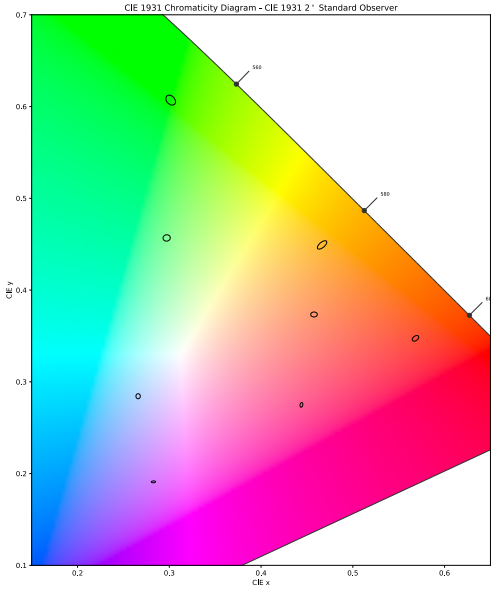

Figure 4.18: Ellipses fitted on the data subjected to the reevaluation using JETI Spectraval 1511 HiRes 4.14; Plotted in the CIE 1931 xy diagram.

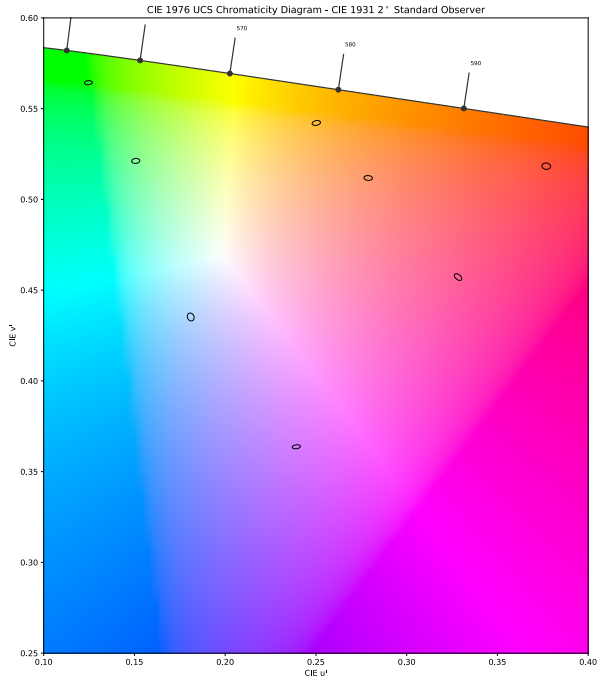

Figure 4.19: Ellipses fitted on the data subjected to the reevaluation using JETI Spectraval 1511 HiResv 4.15; Plotted in the CIE 1976 u'v' diagram.

As a part of the tool performance evaluation under the conditions set in the Phase 2 we have once again computed the mean and the median colour difference values using the metrics mentioned in the Phase 1 (see 4.2):

Colour center number	Mean ΔE_{94}	Median ΔE_{94}	Mean ΔE_{00}	Median ΔE_{00}
1	0.371	0.302	0.337	0.276
2	0.372	0.229	0.431	0.248
3	0.380	0.246	0.436	0.280
4 (Cherry)	0.442	0.409	0.414	0.391
5 (Violet)	0.342	0.261	0.329	0.252
6	0.360	0.262	0.337	0.240
7 (Green)	0.519	0.313	0.689	0.367
8 (Red)	0.411	0.332	0.437	0.347

Table 4.4: The mean and the median ΔE_{00}, ΔE_{94} values of the indistinguishable points obtained during the experiment, phase 2.

The computation results shown in the Tab. 4.4 indicate that in the contrary to the first experiment (see Tab. 4.2) violet area colours became harder to distinguish between (samples 4-5), which resulted in higher. However chromatically saturated colours maintained their position as the most indistinguishable (samples 7-8).

As before, the parameters of the physically attained colour centres displayed during the second phase of the test are presented the Tab. 4.5:

#	L^*	a^*	b^*
1	45.564	-66.011	61.739
2	48.621	3.664	57.991
3	46.570	68.100	54.994
4	48.339	59.822	4.069
5	48.727	56.771	-60.224
6	49.184	-39.540	27.966
7	48.402	-5.477	-14.009
8	47.996	25.943	32.666

Table 4.5: CIE L*a*b* coordinates of the predefined tested colours (see Tab.4.1) subject to remeasurement using JETI Spectraval after the second phase of the experiment.

Values stated in the Tab. 4.3 correspond with the measuring specifications of the spectroradiometer (see Appendix A) and, along with the visual outputs, prove the stability and precision of the implemented instrument in the photopic range.

4.4 Experiment: Phase 3

The last phase of the experiment where an attempt was taken to achieve mesopic conditions and the proposed tool to the proof under them.

Filter choice

In the final phase of the pilot experiment we aimed to achieve conditions that could be considered mesopic [29, 36]. To reach these lighting levels, we expanded the experimental setup by introducing filtering materials, since such have already been used for colourimetric psychovisual experiments [13]. The options we considered included using photographic filters and filtering foils. Both types were ideally supposed to be chromatically neutral, meaning they should not change the colour of the sample displayed on the screen but merely reduce its brightness.

The filter closest to this ideal is a neutral density (gray) photographic filter. We measured an optical transmittance, i.e. a dimensionless quantity that describes the ratio of the transmitted and the received radiant flux, of one of such [16] using a halogen lamp as a reference light source and the above mentioned JETI Spectraval 1511 HiRes. First, we measured the emission spectrum of the halogen lamp reflected from a white surface within the range of 380-780 nm with a step of 1 nm. Then we conducted a similar measurement with the filter. The data from the reference and filtered spectra were smoothed using a moving average to eliminate noise. The result is presented in Fig. 4.20.

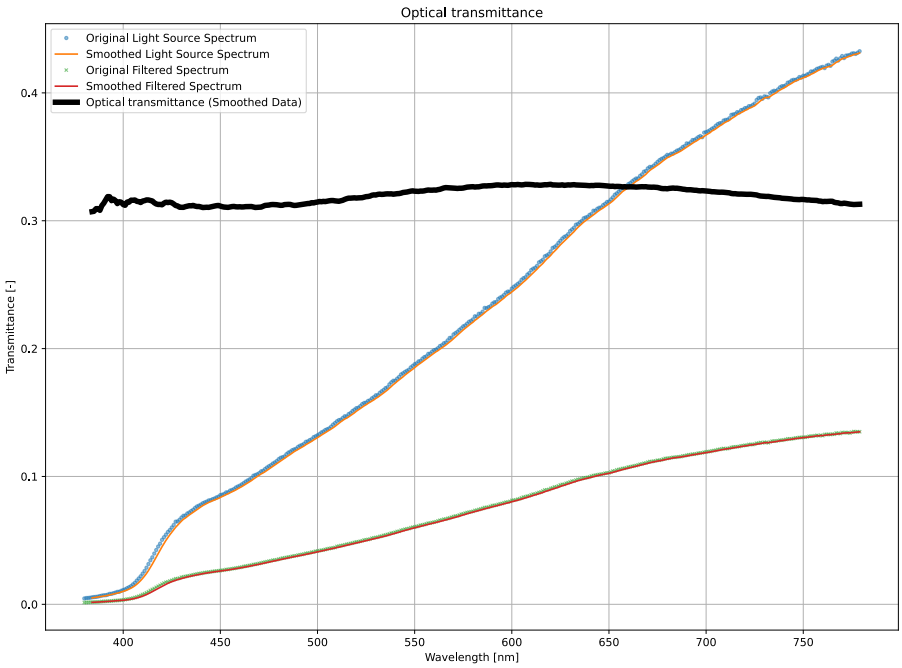

Figure 4.20: Optical transmittance of a photographic neutral density filter HOYA Prond 2 [16].

The filter has demonstrated relatively flat transmittance function throughout the whole visible spectrum. Nevertheless, its transmittance amplitude obviously did not guarantee reaching mesopic luminance conditions even given 40 cd/m^2 monitor calibration. Also, the size of the filter ($d = 8.2$ cm) did not allow for conducting the experiment with observers, as the filter is geometrically designed to be used on a lens, which would complicate its placement on a headrest (or any other placement method above the subject) and sequential placement in front of the spectroradiometer for measuring physically achieved values.

Finally, remeasurement of the obtained values is recommended even considering the fact that the filter's transmittance does not exhibit strong chromatic shifts, so our final choice was combining multiple neuter density foils.

Two connected foils were subjected to a similar experiment as described above. The result is presented in Fig. 4.21.

Though having significantly worse transmittance function, the foils allowed for lowering the luminance levels to the extent where we could consider the conditions to be mesopic [29, 36]. In addition, the use of the foils allowed us to evenly distribute the filtering material over the entire screen area and achieve more uniform displaying conditions.

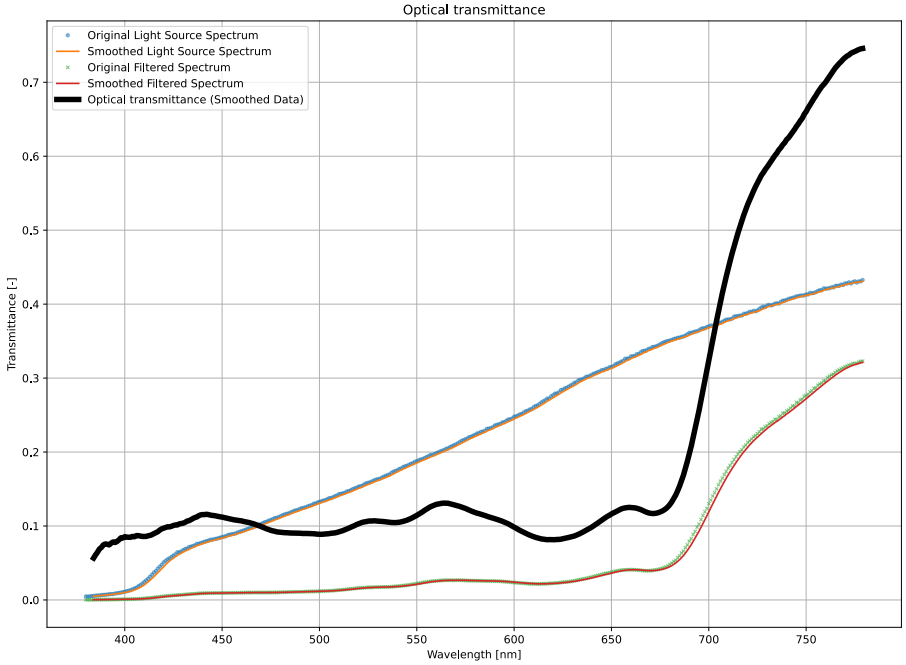

Figure 4.21: Optical transmittance of the two connected neutral density ROSCO 3403 N.6 foils (for foil specification see [27]).

4.4.1 Measurement results

Due to the performance restriction of the spectroradiometer we have used it was decided to reduce the number of the subjects as well as the number of testing directions and tested colour centres. Our intent was not to conduct a comprehensive measurement, but rather to demonstrate, by conducting a pilot experiment, the capability of the proposed tool to handle such a measurement.

In the third phase four colour centres out of 8 initial colours (see Tab. 4.1). The colour coordinates in CIE L*a*b* are presented in Tab. 4.6.

#	L^*	a^*	b^*
1	76.069	-65.163	62.132
2	76.069	4.757	58.180
3	76.069	61.071	4.258
4	76.069	-5.928	-14.477

Table 4.6: CIE L*a*b* coordinates of the predefined tested colours used in the third phase of the pilot experiment.

The third phase of the experiment was held with the monitor calibrated on 40 cd/m^2 and the two connected foils, as was mentioned above, distributed over the entire screen. The results of this phase of the experiment are presented below:

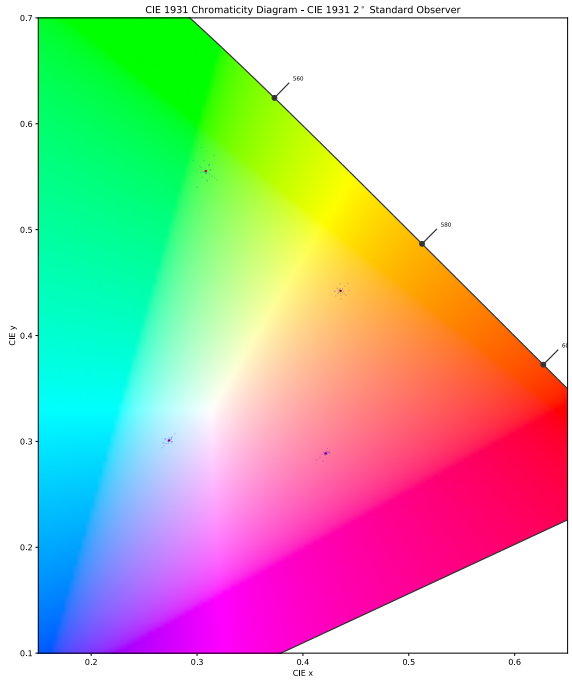

Figure 4.22: Values obtained in the third phase of the experiment for the monitor calibrated on 40 cd/m^2 luminance level with two foils; Plotted in CIE 1931 xy diagram.

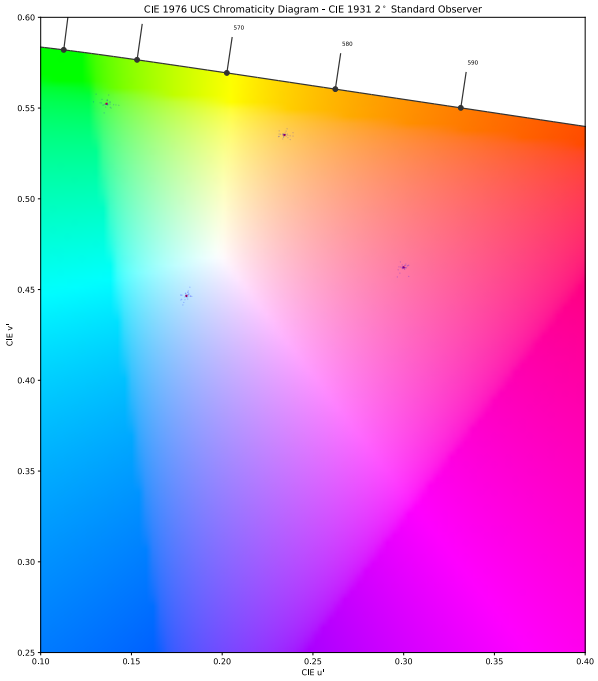

Figure 4.23: Values obtained in the third phase of the experiment for the monitor calibrated on 40 cd/m^2 luminance level; Plotted in CIE 1976 u'v' diagram.

In 4.22 and 4.23 the results of the colour matching test held under mesopic conditions are presented.

These results show significant expansion of the data across all the tested colour centres (For reference see figures: 4.4, 4.5, 4.12, 4.13).

Here we also enclose (as in both previous sections: see Phase 1 4.2, Phase 2 4.3) the physically attained colours, or in other words the distribution of the samples that were really presented to the observers through the foils:

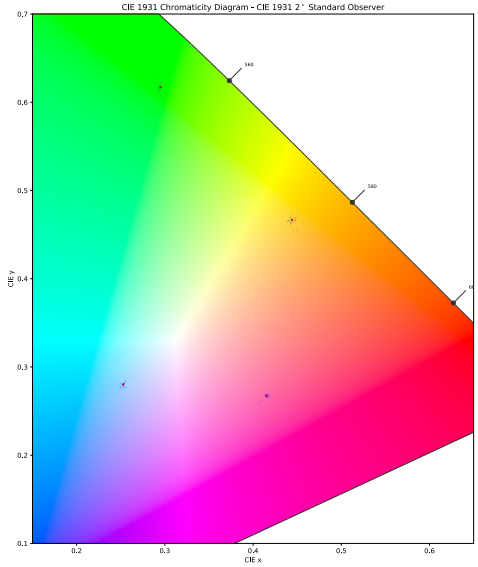

Figure 4.24: Remeasured values from the third phase of the experiment 4.22; Plotted in the CIE 1931 xy diagram.

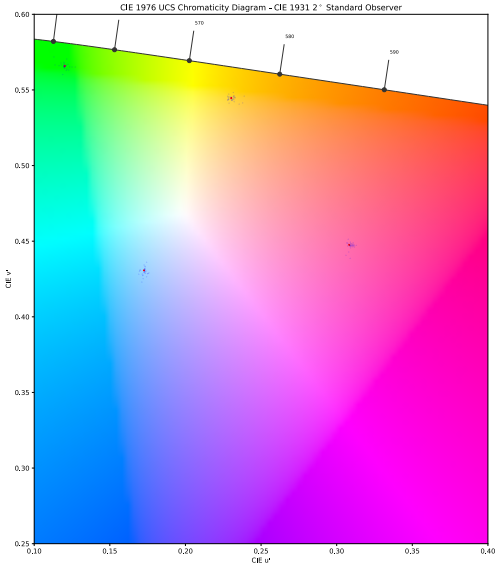

Figure 4.25: Remeasured values from the third phase of the experiment 4.23; Plotted in the CIE 1976 u'v' diagram.

A serious chromatic shift is evident in the Fig. 4.24, 4.25 in relation to the data distribution from the Fig. 4.22, 4.23. This is of course due to the curved shape of the transmittance function of the used foils (see Fig. 4.21).

Given this fact, in this section we only find it relevant to enclose the ellipses fitted on the data subjected to the reevaluation. The fit is presented in the Fig. 4.26 and Fig. 4.27:

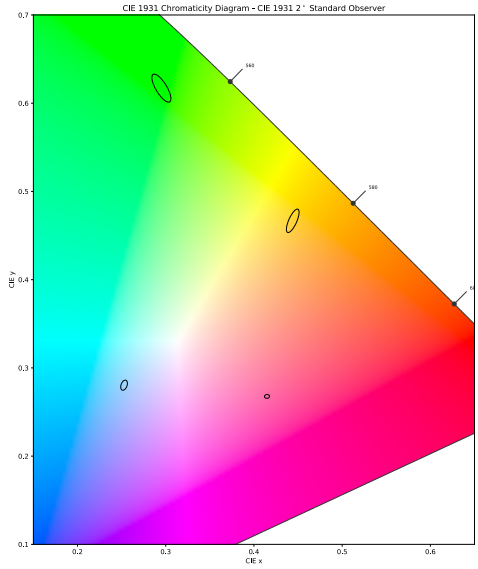

Figure 4.26: Ellipses fitted on the data from the third phase subjected to the reevaluation using JETI Spectraval 1511 HiRes 4.24; Plotted in the CIE 1931 xy diagram.

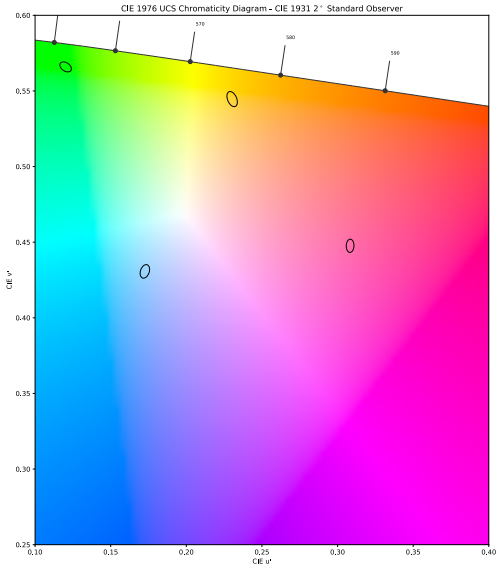

Figure 4.27: Ellipses fitted on the data subjected to the reevaluation using JETI Spectraval 1511 HiResv 4.25; Plotted in the CIE 1976 u'v' diagram.

Once again the mean and the median colour difference values in the population of the points obtained in the third phase of the pilot experiment were computed using the metrics mentioned above (see Tab. 4.2, Tab. 4.4):

Colour center number	Mean ΔE_{94}	Median ΔE_{94}	Mean ΔE_{00}	Median ΔE_{00}
1 (Blue)	0.489	0.409	0.424	0.344
2 (Orange)	0.459	0.378	0.542	0.416
3 (Cherry)	0.498	0.383	0.358	0.266
4 (Green)	0.534	0.474	0.624	0.498

Table 4.7: The mean and the median $\Delta E_{00}, \Delta E_{94}$ values of the indistinguishable points obtained during the experiment, phase 3.

Colour center number	Mean Y (cd/m^2)
1 (Blue)	1.786
2 (Orange)	1.676
3 (Cherry)	1.614
4 (Green)	1.726

Table 4.8: Mean tristimulus CIE Y values of the samples related to each colour center.

The luminance levels remeasured during the final evaluation stage of this phase of the experiment were averaged across all points and written down in the table (see. Tab. 4.8). The mean Y values obtained during this phase indicate that mesopic conditions have actually been achieved across all the presented stimuli, since mesopic range of CIE Y is approximately 0.005 to 5 cd/m^2 [29].

The values of the colour centres obtained after the reevaluation are presented below (see Tab. 4.9):

#	L^*	a^*	b^*
1	16.104	-71.443	59.823
2	16.382	6.889	60.097
3	16.649	67.221	8.307
4	16.722	-9.292	-19.003

Table 4.9: CIE L*a*b* coordinates of the predefined tested colours used in the third phase of the pilot experiment (see Tab. 4.6) subject to remeasurement using the JETI Spectraval spectroradiometer.

As seen from Tab. 4.9, in the mesopic range, the chromaticity distortion between the passed in and the observed colours is the biggest out of all

observed luminance levels, which might be due to the physical restrictions of the spectroradiometer.

The computation results shown in the Tab. 4.7 exhibit a significant increase in the colour difference between the points marked by the subjects as indistinguishable from each other. This corresponds well with the very evident expansion of the ellipses fitted on the data.

Both visual and computational output of the conducted experiment correspond with the findings introduced in the practical part of the thesis,i.e. in the mesopic vision there is a weaker cone cells' response to the presented stimuli. In other words, less colour is perceived by the HVS and more rods are engaged in the vision process, which resulted in the chromaticity difference ellipses extension. What is also noteworthy is that the ellipses in the third part of the experiment did not exhibit any major rotation angle change in comparison with the ones presented in first and the second phases of the experiment (see Phase 1 4.2, Phase 2 4.3, Fig. 4.28). That indicates that the directions, in which it is more or less difficult to distinguish the presented sample from the colour center it is related to, does not demonstrate any major luminance dependence.

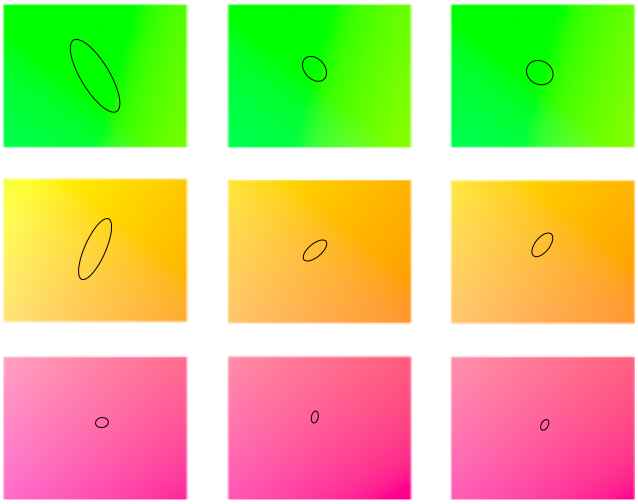

Figure 4.28: An illustrative comparison of the chromaticity discrimination ellipses drawn with our tool for three different levels of luminance. The ellipses are arranged in order of increasing luminance.

Chapter 5

Conclusion and possible future expansions

In the course of working on this thesis, we analyzed the literature dedicated to various characteristics of the human visual system (HVS) and the possibilities of measuring them through various psychophysical experiments. The main part of the thesis was devoted to measuring the response of the HVS to colourimetric changes in a visual stimulus under different lighting conditions.

In the practical part, we developed a tool that allows conducting psychophysical experiments with a group of observers to identify the HVS's ability to differentiate between a provided group of colours. This tool provides a visually comprehensible output in the form of chromatic ellipses plotted in the CIE diagrams, delimiting the group of colours indistinguishable from a given colour center. During the pilot experiment with a group of observers, the functionality of this tool and the correspondence of its outputs to the theoretical basis described in the first part of the Bachelor's thesis were verified.

During the pilot experiment, in one of its phases, we attempted to measure the HVS's response to colour changes under mesopic conditions. For this purpose, filtering foils were used to reduce the brightness level.

A further improvement/expansion of the experiment could involve using higher quality filters (the ones that were also described in the practical part) to achieve less colour distortion across the entire spectrum. Our choice was constrained by time and economical limitations, as well as the fact that conducting the most precise measurements in the mesopic range was not the primary goal of the thesis. Another improvement in conducting the experiment could be the selection of a more suitable colour gamut. In our experiment, we used ITU-R Recommendation BT.2020 as the widest possible variation, however, this led to slight distortions in the displayed samples, particularly in highly saturated areas.

A drawback of the presented tool is also that while measuring the response of the HVS to the colourimetric change in the presented stimuli it can not define different types of colour vision deficiencies, as some commercial devices, as it was discussed in the theoretical introduction 2.3.2. On the contrary, the advantage of the proposed system is in that it provides much more flexibility in choosing the visual angle, under which the experiment is conducted, the set

of the tested samples and, what is more important, unlike many commercial devices allows for testing colours from different parts of the colour spectrum in one session.

Considering all of the said above, we believe that this thesis can serve as a good foundation for future theoretical and practical work on this topic. The developed tool can be used for studying colour and colour perception as well as for conducting larger-scale tests with a bigger group of participants.

Bibliography

[1] G. B. Arden and J. J. Jacobson. "A simple grating test for contrast sensitivity: preliminary results indicate value in screening for glaucoma." In: *Investigative Ophthalmology Visual Science* 17.1 (Jan. 1978), pp. 23–32. ISSN: 1552-5783.

[2] J. Bosten. "Do You See What I See? Diversity in Human Color Perception". In: *Annual Review of Vision Science* 8 (Sept. 2022). DOI: 10.1146/annurev-vision-093020-112820.

[3] L. Brun and A. Tremeau. "Digital Color Imaging Handbook". In: *Color Research and Application - COLOR RES APPL* 29 (Jan. 2002), pp. 589–637.

[4] C. Bulens et al. "Contrast sensitivity in Parkinson's disease". In: *Neurology* 36.8 (1986), pp. 1121–1121. DOI: 10.1212/WNL.36.8.1121.

[5] CIE. *CIE 1976 L*a*b* Colour Space*. 2020. URL: https://cie.co.at/eilvterm/17-23-076 (visited on 05/11/2024).

[6] A. Colenbrander. "The Historical Evolution of Visual Acuity Measurement". In: *Vis Impair Res* 10 (Aug. 2009), pp. 57–66. DOI: 10.1080/13882350802632401.

[7] Wikimedia Commons. *1931 CIE chromaticity diagram showing some RGB color spaces as defined by their chromaticity triangles*. 2014. URL: https://en.wikipedia.org/wiki/RGB_color_spaces#/media/File:CIE1931xy_gamut_comparison.svg (visited on 05/11/2024).

[8] Wikimedia Commons. *CIELAB chroma*. 2023. URL: https://commons.wikimedia.org/wiki/File:CIELAB_chroma.svg (visited on 05/11/2024).

[9] Eizo Corporation. *EIZO ColorEdge 318-4k specifications and documentation*. May 2024. URL: https://www.eizo.com/prodeizo/media/contentassets/2019/03/25/UM-03V25351D1-EN.pdf.

[10] Eizo Corporation. *EIZO ColorNavigator7 specifications and documentation*. May 2024. URL: https://www.eizoglobal.com/support/db/files/manuals/00N0N488AZ/UM-CN7-en-US-00N0N488AZ.pdf.

[11] J. Dahl. *CIELAB chroma*. 2008. URL: https://upload.wikimedia.org/wikipedia/commons/9/9f/Snellen_chart.svg (visited on 05/12/2024).

[12] S. Farrell, S. Daly, and T. Kunkel. "A Cinema Luminance Range by the People, for the People: Viewer Preferences on Luminance Limits for a Large Screen Environment". In: *SMPTE Motion Imaging Journal* 124 (Oct. 2014). DOI: 10.5594/j18577.

[13] D. de Fez, M. J. Luque, and V. Viqueira Pérez. "Enhancement of Contrast Sensitivity and Losses of Chromatic Discrimination with Tinted Lenses". In: *Optometry and vision science : official publication of the American Academy of Optometry* 79 (Oct. 2002). DOI: 10.1097/00006324-200209000-00010.

[14] JETI Technische Instrumente GmbH. *JETI Spectraval 1511 HiRes specifications and documentation*. May 2024. URL: https://www.jeti.com/files/content/support/downloads/spectraval%5C%201511.pdf.

[15] L. Halonenn et al. "CIE 191: 2010 recommended system for mesopic photometry based on visual performance". In: (Jan. 2010), p. 73.

[16] HOYA. *HOYA PROND 2*. 2024. URL: https://hoyafilter.com/product/prond2/#specifications (visited on 05/20/2024).

[17] M. Huang et al. "Testing uniform colour spaces and colour-difference formulae using printed samples". In: *Color Research Application* 37 (Oct. 2012). DOI: 10.1002/col.20689.

[18] M. Luo et al. "A comprehensive test of colour-difference formulae and uniform colour spaces using available visual datasets". In: *Color Research Application* 48 (Feb. 2023). DOI: 10.1002/col.22844.

[19] D. L. MacAdam. "Visual Sensitivities to Color Differences in Daylight∗". In: *J. Opt. Soc. Am.* 32.5 (May 1942), pp. 247–274. DOI: 10.1364/JOSA.32.000247.

[20] T. Nagai, K. Kakuta, and Y. Yamauchi. "Luminance dependency of perceived color shift after color contrast adaptation caused by higher-order color channels". In: *Journal of Vision* 22.7 (June 2022), p. 8. ISSN: 1534-7362. DOI: 10.1167/jov.22.7.8.

[21] Q. Pan and S. Westland. "Comparative Evaluation of Color Differences between Color Palettes". In: *Color and Imaging Conference* 2018 (Nov. 2018), pp. 110–115. DOI: 10.2352/ISSN.2169-2629.2018.26.110.

[22] D. Pascale. "A Review of RGB Color Spaces". In: (2003). URL: https://api.semanticscholar.org/CorpusID:15214629.

[23] D. G. Pelli, J. G. Robson, and A. J. Wilkins. "The design of a new letter chart for measuring contrast sensitivity". In: *Clinical Vision Sciences* 2.3 (1988), pp. 187–199. ISSN: 0887-6169.

[24] V. Peruri et al. "Detecting Outliers in High Dimensional Data Sets Using Z-Score Methodology". In: *International Journal of Innovative Technology and Exploring Engineering* 9.1 (Nov. 2019), pp. 48–53. DOI: 10.35940/ijitee.a3910.119119.

[25] J. Richman et al. “Importance of Visual Acuity and Contrast Sensitivity in Patients With Glaucoma”. In: *Archives of Ophthalmology* 128.12 (Dec. 2010), pp. 1576–1582. ISSN: 0003-9950. DOI: 10.1001/archophthalmol.2010.275.

[26] S. L. Risacher et al. “Visual contrast sensitivity in Alzheimer’s disease, mild cognitive impairment, and older adults with cognitive complaints”. In: *Neurobiology of Aging* 34.4 (2013), pp. 1133–1144. ISSN: 0197-4580. DOI: https://doi.org/10.1016/j.neurobiolaging.2012.08.007.

[27] Rosco. *3403 N.6 filter secification*. 2024. URL: https://legacy.rosco.com/mycolor/SED.cfm?titleName=R3403:%20Rosco%20N.6&imageName=../images/filters/Cinegel/3403.jpg (visited on 05/20/2024).

[28] L. Sloan. “Comparison of the Nagel Anomaloscope and a Dichroic Filter Anomaloscope”. In: *Journal of The Optical Society of America* 40 (Jan. 1950). DOI: 10.1364/JOSA.40.000041.

[29] A. Stockman and L. T. Sharpe. “Into the twilight zone: the complexities of mesopic vision and luminous efficiency”. In: *Ophthalmic and Physiological Optics* 26.3 (2006), pp. 225–239. DOI: https://doi.org/10.1111/j.1475-1313.2006.00325.x.

[30] S. Triantaphillidou et al. “Contrast sensitivity in images of natural scenes”. In: *Signal Processing: Image Communication* 75 (2019), pp. 64–75. ISSN: 0923-5965. DOI: https://doi.org/10.1016/j.image.2019.03.002.

[31] S. Wen. “A color difference metric based on the chromaticity discrimination ellipses”. In: *Opt. Express* 20.24 (Nov. 2012), pp. 26441–26447. DOI: 10.1364/OE.20.026441.

[32] Wikipedia contributors. *Visual acuity – Wikipedia, The Free Encyclopedia*. 2024. URL: https://en.wikipedia.org/w/index.php?title=Visual_acuity&oldid=1220938446 (visited on 05/12/2024).

[33] G. Wyszecki and W. Stiles. “Color Science: Concepts and Methods, Quantitative Data and Formulae, 2nd Edition”. In: *Color Science: Concepts and Methods, Quantitative Data and Formulae, 2nd Edition, by Gunther Wyszecki, W. S. Stiles* (July 2000), p. 968.

[34] Q. Xu et al. “Assessing Colour Differences under a Wide Range of Luminance Levels Using Surface and Display Colours”. In: *Color and Imaging Conference* 2019 (Oct. 2019), pp. 355–359. DOI: 10.2352/issn.2169-2629.2019.27.64.

[35] Q. Xu et al. “Testing uniform colour spaces using colour differences of a wide colour gamut”. In: *Opt. Express* 29.5 (Mar. 2021), pp. 7778–7793. DOI: 10.1364/OE.413985.

[36] A. J. Zele and D. Cao. “Vision under mesopic and scotopic illumination”. In: *Frontiers in Psychology* 5 (2015). DOI: 10.3389/fpsyg.2014.01594.

[37] F. Zhang et al. “Cone photoreceptor classification in the living human eye from photostimulation-induced phase dynamics”. In: *Proceedings of the National Academy of Sciences* 116 (Apr. 2019), p. 201816360. DOI: 10.1073/pnas.1816360116.

Appendix A

Technical Specifications

Model Variations	CG318-4K
Panel	
Type	IPS
Backlight	Wide-Gamut LED
Size	31.1" / 79 cm
Native Resolution	4096 x 2160 (17:9 aspect ratio)
Viewable Image Size (H x V)	698.0 x 368.1 mm
Pixel Pitch	0.170 x 0.170 mm
Pixel Density	149 ppi
Grayscale Tones	DisplayPort, HDMI: 1,024 tones (a palette of 65 thousand tones)
Display Colors	DisplayPort, HDMI: 1.07 billion from a palette of 278 trillion
Brightness (typical)	350 cd/m^2
Recommended Brightness for Calibration	120 cd/m^2 or less
Contrast Ratio (typical)	1500:1
HDR Gamma	HLG, PQ curve (optional)
Color Gamut (typical)	Adobe RGB: 99%, DCI-P3: 98%
Built-in Calibration Sensor	Yes

Table A.1: Specifications of the EIZO ColorEdge CG318-4K.

Optical Parameters	
Spectral range	380 ... 780 nm 380 ... 1000 nm (version: spectraval 1511NIR)
Optical bandwidth	4.5 nm 2 nm (version: spectraval 1511HiRes)
Wavelength resolution	1 nm
Digital electronic resolution	16 bit ADC
Viewing angle	1.8
Measuring distance/diameter (measured from front end of the device)	20 cm - Ø 8 mm; 100 cm - Ø 33 mm
Measuring Values	
	Spectral Radiance, Luminance, total Radiance x,y, u',v', CCT, color purity, CRI, RGB and others Spectral Irradiance/Integral Irradiance/Illuminance
With Optional Diffusor	
Measuring Ranges and Typical Measuring Uncertainties	
Luminance measuring range	0.2 ... 180 000 cd/m^2 (Illuminant A) 0.2 ... 140 000 cd/m^2 (typical warm white LED)
Luminance uncertainty	± 4.4% (Illuminant A @ 100 cd/m^2, k = 2)
Luminance repeatability	± 1% (Illuminant A)
Chromaticity uncertainty	± 0.002 x, y (Illuminant A, k = 2)
Color repeatability	± 0.0005 x, y (Illuminant A)
CCT repeatability	± 20 K (Illuminant A)
Max. wavelength error	± 0.2 nm (HgAr line source)
Polarization error f_8	< 2 %

Table A.2: Specifications of the JETI Spectraval 1511 HiRes.

Appendix B

List of attachments

- *colour_matching_test.py* – the main script that performs a psychovisual test explained in the thesis.
- *colour_fidelity_test.py* – the script used in the *colour_matching_test.py* to allow for manual samples fidelity check before the testing begins.
- *final_evaluation.py* – the script, that runs an automatic remeasurement of all the samples retrieved after the testing.
- *results_plot_nonRemeasured.py* – the script for plotting the results non-subject to remeasurement using *final_evaluation.py*.
- *results_plot_Remeasured.py* – the script for plotting the results subject remeasurement using *final_evaluation.py*.
- *results* – the directory where all the results for all the observers are saved in a form of CSV tables after the testing.
- *finalEval* – the directory where the aggregated data on every sample retrieved from the testing and every colour centre is saved in a form of one CSV table.
- *colourpicker* – the directory containing special colour picker used during the pilot experiment for picking values inside the physically feasible gamut.
- *colourpicker.py* – the script itself, placed in *colourpicker* directory.

Appendix C

Used devices' and other illustrations, final remarks

Figure C.1: An illustration of Eizo ColorEdge CG318-4K monitor with the inbuilt calibration sensor (taken from the manufacturer web-site).

Figure C.2: An illustration of JETI Spectraval 1511 HiRes with the stray-light protection tube (taken from the manufacturer web-site).

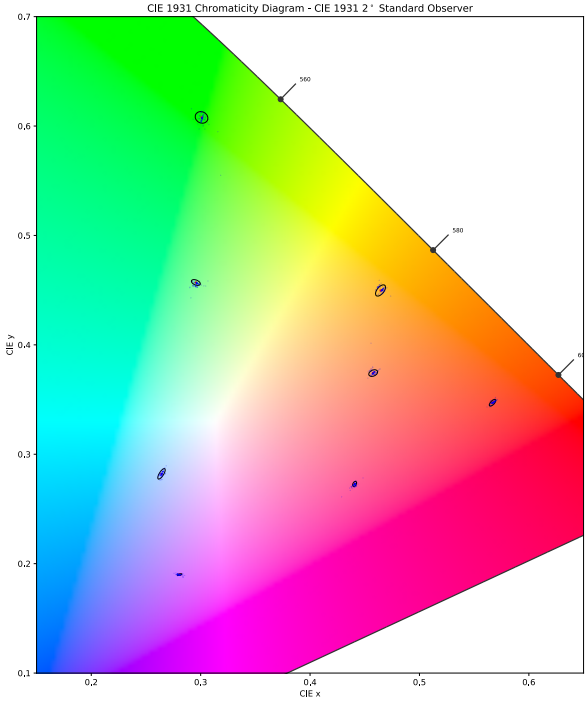

Figure C.3: Complete data drawing illustration for the first phase of the experiment.

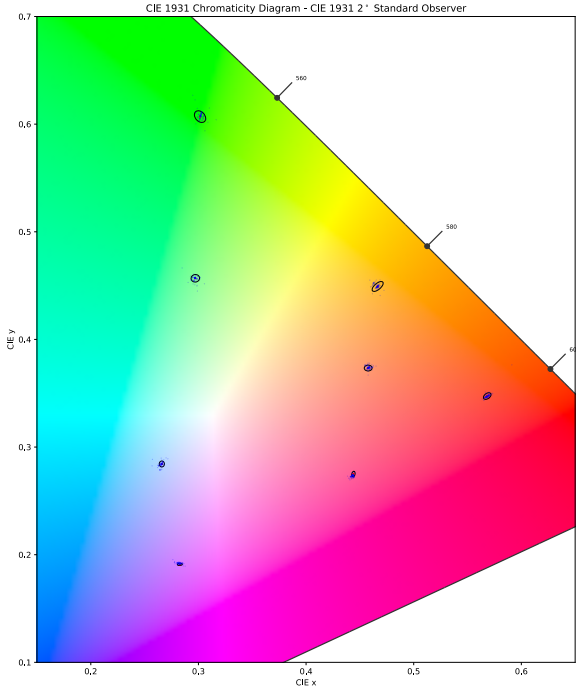

Figure C.4: Complete data drawing illustration for the second phase of the experiment.

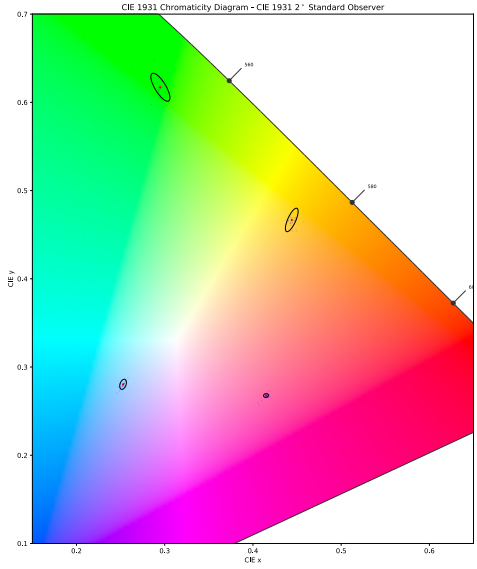

Figure C.5: Complete data drawing illustration for the third phase of the experiment.

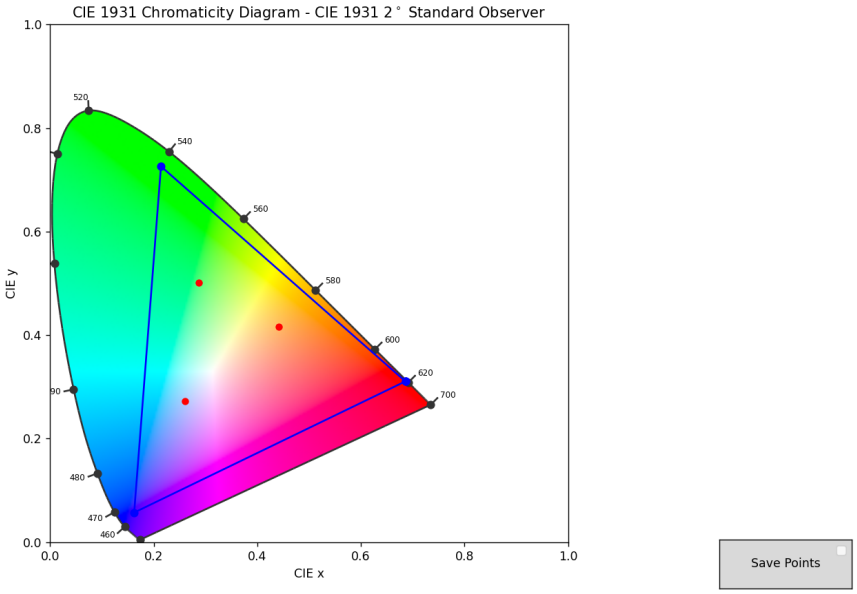

Figure C.6: An interface of the colourpicker proposed in the empirical part of the experiment to test the samples laying strictly inside of the physically feasible ITU-R BT.2020 gamut.

Here I would also like to notify, that in some parts of this thesis, e.g. for sentences reformulation and other appropriate purposes, artificial intelligence tools were used, such as ChatGPT by OpenAI. All in accordance with the CTU Methodological guideline ČVUT MP 2023 V02.